



ALMA MATER STUDIORUM  
UNIVERSITÀ DI BOLOGNA

**DOTTORATO DI RICERCA IN**  
**Biologia Cellulare e Molecolare**

Ciclo XXXVI

**Settore Concorsuale: 05/E2 – Biologia Molecolare**

**Settore Scientifico Disciplinare: BIO/11 – Biologia molecolare**

**EBV Type II latency relies on PARP1 activity and is essential for  
gastric epithelial cell transformation in EBV-associated Gastric  
Cancer (EBVaGC)**

**Presentata da: Davide Maestri**

**Coordinatore Dottorato**

**Prof. Vincenzo Scarlato**

**Supervisore**

**Prof. Giovanni Perini**

**Co-supervisore**

**Italo Tempera, PhD**

Esame finale anno 2024

## Abstract

Epstein-Barr virus (EBV) establishes a lifelong asymptomatic infection by replicating its chromatinized genome, called episome, together with the host genome. EBV exhibits different latency-associated transcriptional repertoires that mirror its three-dimensional structures of the genome. CTCF, Cohesin and PARP1 are involved in maintaining viral latency and establishing episome architecture. Epstein-Barr virus-associated gastric cancer (EBVaGC) represents almost 10% of all gastric cancers globally. EBVaGC exhibit an intermediate viral transcription profile known as "Latency II", expressing specific viral genes and non-coding RNAs. In this study, we investigated the impact of PARP1 inhibition on CTCF/Cohesin binding in Type II latency. We observed a destabilization of the binding of both factors, leading to a disrupted three-dimensional architecture of the episomes and consequently, an altered viral gene expression. Despite sharing the same CTCF binding profile, Type I, II, and III latencies display different 3D episomal structures that correlate with variations in viral gene expression. Additionally, our analysis of H3K27ac-enriched chromatin interactions revealed differences between Type II latency episomes and a link to cellular transformation through docking of the EBV episomes at specific sites of the Human genome, thus promoting oncogene expression. Overall, this work provides insights into the role of PARP1 in maintaining active latency and novel mechanisms of EBV-induced cellular transformation.

# Index

1. Introduction	3
1.1 Epstein-Barr virus (EBV) and latency	3
1.2 Epigenetic regulation of viral gene expression	5
1.3 Regulation of viral gene expression thorough CTCF and Cohesin binding	6
1.4 CTCF/Cohesin complex role in regulating the viral chromatin architecture	8
1.5 Poly (ADP-ribose) Polymerase 1 (PARP1) is involved in latency maintenance	10
1.6 EBV associated Gastric Cancers (EBVaGC)	11
1.7 EBVaGC cellular models	13
2. Aim of the study	14
3. Results	15
3.1 The three-dimensional architecture of the viral genome is different in all latency types and mirrors viral gene expression	15
3.2 PARP1 inhibition alters CTCF/Cohesin binding and viral chromatin looping	19
3.3 PARPi affects viral gene expression	25
3.4 CTCF occupies viral regions with an enhancer epigenetic signature	30
3.5 HiChIP analysis reveals distinct three-dimensional structures and enhancer interactions in SNU719 and YCCEL1 cell lines	33
3.6 EBV enhancer regions are tethered to specific loci across the host genome	35
3.7 Functional Role of EBV-Human Interactions: Gene Expression Analysis Reveals Strong Viral Enhancers Associated with Gastric Cancers	40
4. Discussion	45
5. Conclusions	50
6. Materials and Methods	51

# 1. Introduction

## 1.1 Epstein-Barr virus (EBV) and latency

Epstein-Barr virus (or EBV) is a human gammaherpesvirus, that infects more than 95% of the adult population (Epstein, Achong, and Barr 1964; Young, Yap, and Murray 2016; Dunmire, Verghese, and Balfour 2018).

EBV infects both epithelial and B cells and subsequently establishing a lifelong asymptomatic condition (Smatti et al. 2018) through the formation of circularized mini-chromosomes known as episomes, which replicate with the host genome. Even though EBV persistent infection is asymptomatic, nearly 140,000 people die annually from untreatable malignancies caused by EBV infection of lymphoid or epithelial cells (Khan and Hashim 2014; Wong et al. 2022), including post-transplant lymphoproliferative disorders (PTLD) (Hsu and Glaser 2000), Burkitt's Lymphoma (BL) (Epstein, Achong, and Barr 1964), Diffuse Large B-cell Lymphoma (DLBCL), gastric carcinomas (GC), and nasopharyngeal carcinoma (NPC) (Shannon-Lowe and Rickinson 2019; Farrell 2019; Thorley-Lawson et al. 2013).

Every infected cell contains multiple episomes tethered to the host chromosomes through the viral transcription factor called EBV Nuclear Antigen 1 (EBNA-1), thus making it essential for EBV to organize its chromatin in a way that allows access to essential genes for transcription and replication while maintaining genomic stability. EBNA-1 tethering of the viral chromosomes to host chromosomes during cell division ensures that in each sister cell at least one copy of EBV is present (Hodin, Najrana, and Yates 2013).

EBV exhibits different latency-associated transcriptional repertoires, each responsible for specific gene expression during different stages of infection and characterized by different three-dimensional structures of the viral genome (Caruso, Maestri, and Tempera 2023; Morgan et al. 2022; Price and Luftig 2015).

EBV can adopt at least three different latency types (Figure 1). Type I latency is characterized by the expression of just the Epstein-Barr virus-encoded small RNAs (EBERs) and EBNA-1, the transcription of which is initiated from the Qp viral promoter

(Woisetschlaeger et al. 1990; Nonkwelo et al. 1996; Trivedi et al. 2001). EBNA-1 is able to self-regulate its expression by binding the Qp promoter which contains two EBNA-1-binding sites (Nonkwelo et al. 1996; Jones, Hayward, and Rawlins 1989; Sample, Henson, and Sample 1992). Type I latency is observed in EBV+ Burkitt Lymphoma tumors, in Burkitt Lymphoma cell lines and in memory B cells from healthy individuals.

In Type II latency, EBV expresses the two Latent Membrane Proteins (LMP2A/B), EBERs and the miRNA BamHI fragment A rightward transcripts (BARTs) in addition to EBNA-1 from the Qp promoter. This type of latency is characteristic of nasopharyngeal carcinoma and Hodgkin disease (HD) cells (Chiang et al. 1996).

In Type III latency, EBV expresses all the latent viral transcripts, consisting of six EBNAs (EBNA-1, -2, -3A, -3B, -3C and -LP), two LMPs (LMP1 and LMP2), and the EBER and BART non-coding RNAs (Thorley-Lawson and Gross 2004). The transcription of the EBNAs, including EBNA-1, is initiated by the Cp promoter (Rowe et al. 1992) which contains an EBNA-2 responsive element upstream of the 5' of TSS. The binding of both EBNA-2 and EBNA-LP upregulates Cp activity, leading to positive autoregulation of EBNA transcripts (Woisetschlaeger et al. 1990; Abbot et al. 1990; Rooney et al. 1992; F. Wang et al. 1987; 1990). Type III latency is observed *in vitro* in proliferating primary B cells after EBV infection and *in vivo* in PTLD and DLBC lymphoma cells (Price and Luftig 2015; Rowe et al. 1992; Brink et al. 1997; Price et al. 2012).

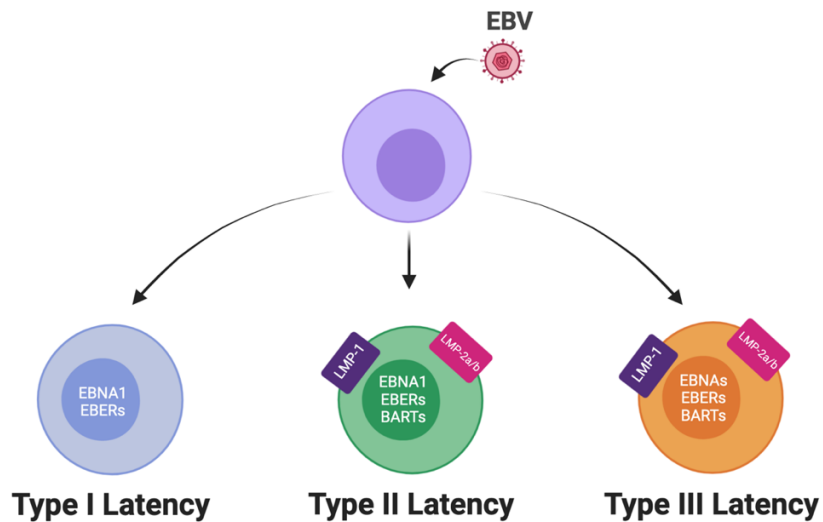


**Figure 1.** Illustration of the three main latency programs. Expressed genes are depicted in the subcellular compartment where they localize (Caruso, Maestri, and Tempera 2023).

## 1.2 Epigenetic regulation of viral gene expression

Viral promoter switching determines which latency state the EBV-infected B cells will adopt (Woisetschlaeger et al. 1990; Takacs et al. 2010). The regulation of viral gene transcription is regulated through viral and host factors, including epigenetic regulators (Buschle and Hammerschmidt 2020; Tempera and Lieberman 2010; 2014). The importance of epigenetic modifications such as methylation of the viral genome, in the regulation of EBV gene expression emerged from early studies. Indeed, treating EBV+ B cells with hypomethylating agents induced EBV viral replication (Masucci et al. 1989; Robertson et al. 1995; Tao et al. 1998; Ambinder, Robertson, and Tao 1999).

Moreover, EBV genome is highly methylated, restricting viral gene expression in both B and epithelial cells (Ambinder, Robertson, and Tao 1999). Analysis of CpG methylation across the EBV genome during *in vitro* infection of primary B cells demonstrated that viral genome methylation is a slow process that requires several weeks post-infection for completion, thus suggesting that other epigenetic and cellular factors may play a fundamental role in the early regulation of viral gene expression (Bergbauer et al. 2010;

Kalla et al. 2010; Kintner and Sugden 1981; Woellmer, Arteaga-Salas, and Hammerschmidt 2012). DNA methylation, instead, may be fundamental in controlling and maintaining viral gene expression in later phases of EBV infection and latency. Consistent with these observations, the degree and distribution of DNA methylation across the EBV genome varies between latency types, with high levels of methylation observed in Type I infected cells, indicating that DNA methylation is an essential epigenetic mechanism for maintaining latency programs (Tempera, Wiedmer, et al. 2010; Falk et al. 1998; Hughes et al. 2012).

Further studies support the notion that each latency type is characterized by a specific viral epigenetic landscape. The deposition of different patterns of histone modifications correlates with different EBV latency types (Tempera, Wiedmer, et al. 2010; Arvey et al. 2012; Arvey, Tempera, and Lieberman 2013). These studies demonstrated that in Type III latency, which is the most permissive type of latency concerning latent viral genes expressed, the EBV genome was highly enriched in histone marks associated with open chromatin and active gene expression, including H3K27ac and H3K4me3. In contrast, in Type I latency, where the EBV gene expression is limited to only EBNA-1, the viral epigenetic landscape is characterized by repressive histone marks such as H3K9me3 and H3K27me3 (Tempera, Wiedmer, et al. 2010; Arvey et al. 2012).

### **1.3 Regulation of viral gene expression thorough CTCF and Cohesin binding**

With the advent of modern chromatin-binding protein profiling techniques such as, Chromatin Immunoprecipitation followed by deep sequencing (ChIP-seq), it has been possible to identify distinct domains of transcriptionally active and inactive regions and new factors which can prevent the spread of one domain to the next. CTCF (CCCTC-binding factor) is a highly conserved zinc finger protein that plays an essential role in chromatin organization and gene regulation (Bell, West, and Felsenfeld 1999; Phillips and Corces 2009). CTCF role in organizing chromatin domains is made possible through its binding to specific DNA sequences known as insulator elements which prevent the spread

of epigenetic modifications, thus maintaining the integrity of gene expression programs (Phillips and Corces 2009).

In recent years, several studies showed the key role of CTCF in the context of EBV infection. In fact, CTCF has been shown to bind to the EBV genome during latency (Tempera, Wiedmer, et al. 2010; Hughes et al. 2012; Chau et al. 2006; Day et al. 2007). ChIP-seq experiments identified at least 17 CTCF binding sites across the EBV genome (Morgan et al. 2022; Arvey et al. 2012; Arvey, Tempera, and Lieberman 2013; Holdorf et al. 2011; Lupey-Green et al. 2017). In particular, CTCF has been shown to bind to the latent promoters Cp, Qp and LMPs, as well as the early lytic promoter Zp of the BZLF1 gene, which encodes for the lytic transactivator Zta (Arvey et al. 2012). Surprisingly, no differences in CTCF binding across the viral genome were found between latency types (Morgan et al. 2022), although between Type III and Type I latency, a difference in the CTCF binding strength at Cp promoter was observed (Chau et al. 2006). Moreover, EBV genomes carrying mutations of CTCF binding sites either at Cp, Qp, or LMPs promoters show impaired gene expression and altered chromatin composition of the neighboring regions (Tempera, Wiedmer, et al. 2010; Chau et al. 2006; Chen et al. 2014). The disruption of CTCF binding at the Qp promoter in Type I latently infected epithelial cells resulted in the spread of H3K9me3 repressive heterochromatin mark and the accumulation of DNA methylation at the Qp region over time, leading to promoter silencing and inhibition of EBNA-1 expression (Tempera, Wiedmer, et al. 2010). Accordingly, it can be proposed that CTCF binding across the EBV genome physically acts as a barrier that prevents the spreading of epigenetic modifications into viral promoter regions, thus maintaining the integrity of latency gene expression programs. In contrast to what was observed for the latent viral promoter, the disruption of CTCF binding to the BZLF1 promoter failed to reactivate lytic infection of EBV and no significant changes in CTCF binding across the viral genome were observed during the early phase of EBV reactivation, suggesting that CTCF binding per se is not sufficient to completely reverse the epigenetic silencing of lytic promoters (Lupey-Green et al. 2017).

CTCF also plays a critical role in regulating gene expression by influencing the three-dimensional structure of chromatin and promoting or inhibiting interactions between enhancer and promoter gene regions (Phillips and Corces 2009). Recently, it has been

discovered that CTCF usually works together with Cohesin to regulate gene expression and chromosome architecture (Degner et al. 2011; 2009; Millau and Gaudreau 2011). Cohesin is a protein complex critical to chromosome segregation during cell division (Nasmyth, Peters, and Uhlmann 2000). Cohesin can form a complex with CTCF at specific intergenic sites to form chromatin loops that bring enhancers and promoters into proximity, thus regulating gene expression (Degner et al. 2011; Kojic et al. 2018). In addition, CTCF binding limits Cohesin effects to specific regions by acting as a barrier to prevent Cohesin from spreading along the chromatin fiber (Mach et al. 2022). Consistent with these observations, in latently infected cells, ChIP-seq experiments revealed that Cohesin binding profile overlaps with the one of CTCF on specific regions of the viral genome, including the Cp, Qp, BZLF1, and LMP1 promoters (Morgan et al. 2022; Arvey et al. 2012; Arvey, Tempera, and Lieberman 2013).

#### **1.4 CTCF/Cohesin complex role in regulating the viral chromatin architecture**

The notion that CTCF and Cohesin regulate chromatin architecture of the genome in higher eukaryotes prompted similar studies to determine how the 3D structure of the EBV genome in latently infected cells is regulated. Earlier studies focusing on the 3D structure of the Cp and Qp regions of the EBV genome demonstrated that these regions adopt alternative 3D chromatin structures between latency types (Tempera, Klichinsky, and Lieberman 2011). For example, in Type III latency, the active Cp promoter forms a chromatin loop with the origin of latent DNA viral replication (Ori P), which also serves as a transcriptional enhancer (Tempera, Klichinsky, and Lieberman 2011; Reisman and Sugden 1986), while in Type I latency, where Cp is repressed and transcription of EBNA-1 is initiated from the Qp promoter, a chromatin loop between Qp and Ori P was observed (Tempera, Klichinsky, and Lieberman 2011) (Figure 2). In addition, in Type III latency, a chromatin loop that brings Ori P close to the LMP1 promoter was observed, indicating that chromatin loop formation is implicated in regulating viral gene expression during EBV latency (Arvey et al. 2012; Chen et al. 2014). All these chromatin loops occur at regions of the EBV genome where CTCF and Cohesin bind, indicating that CTCF and Cohesin actively participate in the formation of chromatin loops across the viral genome. Indeed,

ablation of their binding at either Cp, Qp, or LMP promoters, determines the disruption of loops occurring between these regions and Ori P (Tempera, Klichinsky, and Lieberman 2011; Chen et al. 2014), indicating that CTCF and Cohesin binding is essential for chromatin loop formation between viral genomic regions.

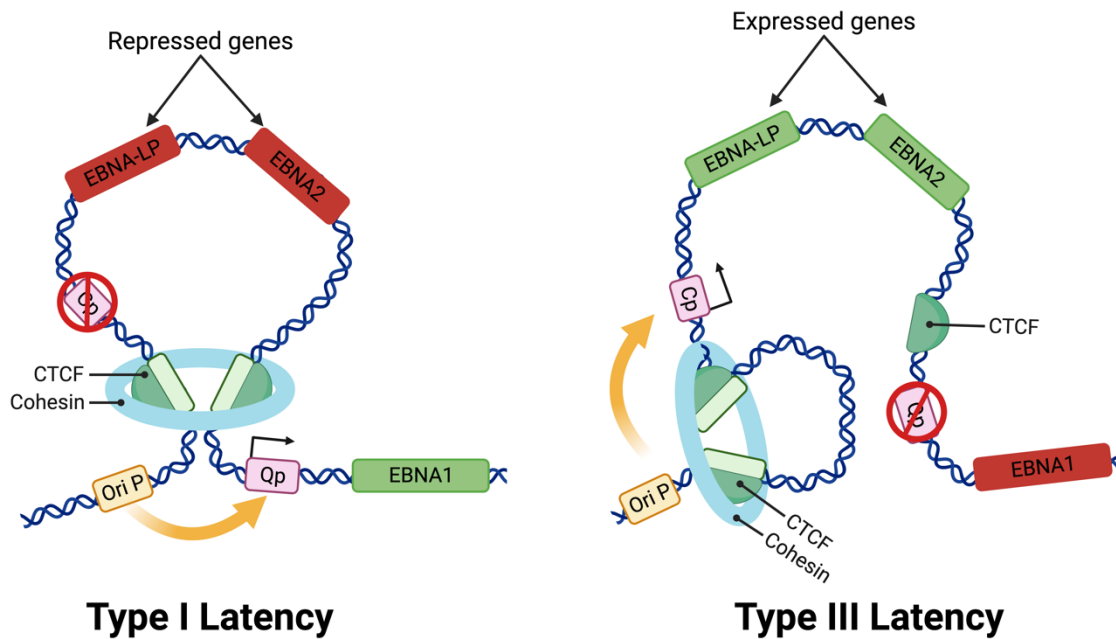


**Figure 2.** Model of viral gene expression regulation through loop formation between Ori P and the active viral promoter (Cp or Qp) in Type I and III latency (Tempera, Klichinsky, and Lieberman 2011) (created with BioRender.com).

Most recently, studies employing EBV-specific Capture-HiC assay revealed the chromatin architecture of the EBV genome in Type I and Type III EBV+ B cells (Morgan et al. 2022). These studies showed several chromatin loops across the viral genome, connecting regulatory DNA elements to viral promoters that contain at least one CTCF binding site (Morgan et al. 2022). From these studies emerged that there is a close correlation between the frequency of chromatin loops, the complexity of 3D structure in EBV latency and the level of transcriptional permissiveness of latent viral genome (Morgan et al. 2022). However, several viral regions are engaged in similar chromatin

loops in both Type I and Type III EBV+ cells. For example, the region upstream of the LMP2 promoter is connected to the regions encoding for the EBERs in both latency types. Similarly, in both Type I and Type III EBV+ cells, a chromatin loop connects the origin of lytic replication OriLyt Left to the CTCF site positioned at the 3' of W repeats, suggesting a potential role of 3D structure in restricting lytic reactivation (Morgan et al. 2022). Moreover, the same region has been proven to form a connection with the Zp lytic promoter through a chromatin loop upon lytic reactivation (Guo et al. 2020).

### **1.5 Poly (ADP-ribose) Polymerase 1 (PARP1) is involved in latency maintenance**

As described above, the EBV genome can assume alternative chromatin architectures that provide an additional layer of epigenetic regulation for EBV gene expression during latent and lytic phases of its lifecycle. Given the central role of CTCF/Cohesin complex in this process, it is striking how the binding profile of this complex across the EBV genome is similar between Type I and Type III EBV+ cells (Morgan et al. 2022). Most recently, this discrepancy in 3D chromatin structures in Type I and Type III EBV+ cells has been attributed, at least in part, to the effect of Poly (ADP-ribose) polymerase 1 (PARP1) on CTCF (Morgan et al. 2022; Lupey-Green et al. 2018). PARP1 catalyzes the apposition of ADP-ribose polymers to acceptor proteins, including histones and CTCF (Messner et al. 2010; Yu et al. 2004; Farrar et al. 2010). PARP1 physically interacts with CTCF, and its PARylation facilitates its functions, including chromatin loop formation (Yu et al. 2004). EBV infection can activate PARP1, in part through the signaling cascade initiated by LMP1 (Martin, Lupey, and Tempera 2016). PARP1 binds to CTCF at specific regions of the EBV genome, and its pharmacological inhibition destabilizes CTCF binding to some regions of the EBV genome (Lupey-Green et al. 2018). In Type III latent B cells, the inhibition of PARP1 ablates viral chromatin architecture which, in turn, causes heterochromatinization of the viral episome and repression of EBV viral genes (Morgan et al. 2022; Lupey-Green et al. 2018) (Figure 3). For example, PARP1 inhibition significantly decreases CTCF occupancy at the Cp promoter and alters the 3D chromatin structure of this promoter region, thus reducing the expression of EBNA2 (Morgan et al. 2022; Lupey-Green et al. 2018). However, only a subset of chromatin loops present

across the EBV genome are affected by PARP1 inhibition, suggesting that other mechanisms, besides PARP1 activity, regulate the EBV tridimensional chromatin structure.

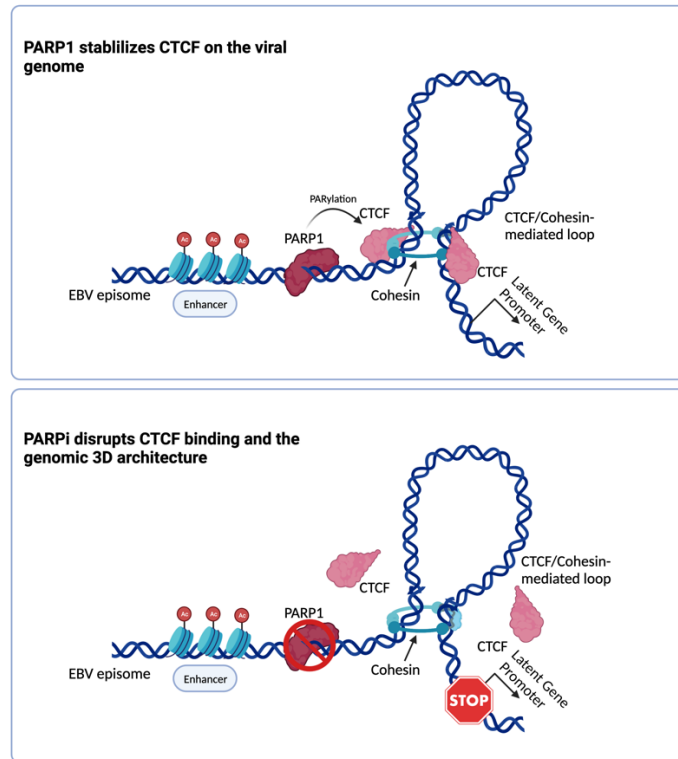


**Figure 3.** Schematic representation of the regulation of the 3D architecture of the viral genome through CTCF/Cohesin/PARP1 axis (Caruso, Maestri, and Tempera 2023).

### 1.6 EBV associated Gastric Cancers (EBVaGC)

Gastric cancers lead to approximately 780,000 deaths every year, making them the third most common cause of cancer-related deaths worldwide (Bray et al. 2018). Among the different types of gastric cancer, Epstein-Barr virus-associated gastric cancer (EBVaGC) is frequently observed (Young and Rickinson 2004). The prevalence of EBVaGC varies based on geographic regions, comprising approximately 1.3% to 30.9% of all gastric cancers (Murphy et al. 2009; Camargo et al. 2011; Naseem et al. 2018; Cristescu et al. 2015), with an overall global average of 8.9% (Murphy et al. 2009). This accounts for approximately 75,000 new cases diagnosed annually (Young and Rickinson 2004).

EBVaGCs consist of monoclonal populations of EBV+ epithelial cells suggesting that infection is an early event in tumorigenesis and a key oncogenic driver (Truong et al. 2009).

EBV-positive gastric cancer is associated with a high prevalence of CpG island hypermethylation (Stanland and Luftig 2020). An hypermethylation of CDKN2A (p16<sup>INK4A</sup>) promoter is characteristic of EBVaGC (Geddert et al. 2010). Other hypermethylated genes include CDH1, PTEN, RASSF1A, MGMT, MINT2, p15INK4B, p73, HOXA10, SSTR1, FHIT, CRPB1, WWOX, DLC1, HOXA11 (The Cancer Genome Atlas Research Network 2014). Moreover, EBVaGC are associated with distinct mutation patterns (K. Wang et al. 2014; 2011). In particular, in EBV+ GC a strong predilection for PIK3CA non-silent mutations has been observed. In addition to PIK3CA mutations, EBVaGC had frequent ARID1A (55%) and BCOR (23%) mutations and only rare TP53 mutations (The Cancer Genome Atlas Research Network 2014).

It is still unclear how EBV infects the cells of the gastric epithelium. It has been hypothesized that after the first infection of epithelial cells of the oral cavity, EBV undergoes multiple cycles of replication and newly formed virions are able to reach the lymphoid tissue and infect naïve B cells. Latently infected B cells that circulate in the blood are able to reach the gut-associated lymphoid tissue (GALT). EBV undergoes lytic replication in the more differentiated and mature cells of the gastric epithelium producing infecting virions. Upon organ injuries due to bacterial infection (*Helicobacter pylori*) or chronic atrophic gastritis, mature cells such as parietal cells are able to re-enter the cell cycle to replace the dead cells. These poorly differentiated cells are targeted by EBV that establishes a Type II latent infection (Stanland and Luftig 2020) (Figure 4).

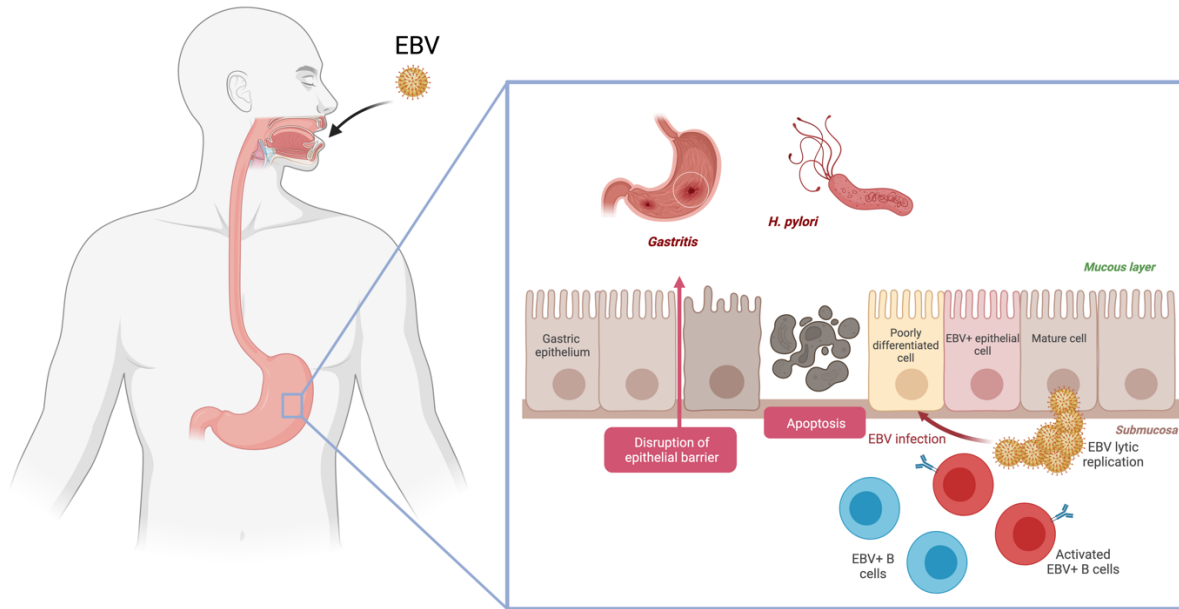


**Figure 4.** Schematic model of EBV infection of gastric epithelial cells (created with BioRender.com).

### 1.7 EBVaGC cellular models

The establishment of the latent infection of gastric tissue *ex vivo* has proven to be challenging and inefficient, making cell lines the most effective way to study EBV infection even though the *in vitro* infection of cancer cell lines and monoclonal non-neoplastic cell lines does not accurately represent the environment in which EBVaGC occurs (Stanland and Luftig 2020).

Therefore, for this project two different EBV+ gastric cancer cell lines were employed: YCCEL1 and SNU719.

Both cell lines were validated for the presence of viral DNA and proteins (Oh et al. 2004; D. N. Kim et al. 2013). From these experiments it was possible to determine that EBV latency is a Type II, consisting in the expression of viral non-coding RNAs, EBNA-1 and LMP2A proteins. Both cell lines show a similar level of EBV copies, even though they have different origin. In particular, SNU719 derive from a solid gastric tumor, while YCCEL1 derive from metastases of an EBVaGC (Oh et al. 2004; D. N. Kim et al. 2013).

## 2. Aim of the study

This research project focuses on studying the correlation between the three-dimensional structure of the Epstein-Barr virus (EBV) genome and the regulation of host gene expression.

EBV was the first oncogenic virus to be identified and is associated with multiple types of blood cancers such as Diffuse Large B-cell Lymphoma (DLBCL), post-transplant lymphoproliferative disorders (PTLD), Burkitt's lymphoma (BL). In addition, despite its tropism for B cells, EBV is also able to infect epithelial cells and cause other types of cancers such as nasopharyngeal carcinoma (NPC) and gastric carcinoma (GC).

All the tumor types listed above are characterized by different types of viral latency each associated to a peculiar 3D structure of the viral genome and a specific gene expression program.

To better understand how the interaction between virus and host is articulated and consequently identify possible therapeutic targets for better treatment of tumors with viral etiology, the following project has two aims:

- 1) The first is to shed light on the dependence of viral latency on PARP1 in EBV-associated Gastric Cancer (EBVaGC);
- 2) The second is to further elucidate the molecular mechanism named 'enhancer infestation' by which EBV could induce cellular transformation by docking at specific sites of the Human genome both altering host epigenetic landscape and serving as an additional enhancer to promote oncogene expression.

### 3. Results

#### 3.1 The three-dimensional architecture of the viral genome is different in all latency types and mirrors viral gene expression

Recent works from our group and others have demonstrated that, following the establishment of latency in infected B cells, the transcription factor CTCF binds to the EBV genome, regulating its gene expression (Tempera, Wiedmer, et al. 2010) (Arvey et al. 2012). Furthermore, in a recent study we identified that, despite the almost unchanged binding of CTCF between Type I and Type III latencies, the three-dimensional (3D) organization of the viral genome is markedly different between the two latency types and is tightly correlated with viral gene expression (Morgan et al. 2022). To evaluate how the binding of CTCF differs between latencies I, III and II, which is typical of EBV-positive gastric tumors, first we conducted a Chromatin Immunoprecipitation followed by sequencing (ChIP-seq) experiment in the two EBV+ gastric cancer (GC) cell lines YCCEL1 and SNU719 and next we compared it with our previously published CTCF ChIP-seq data in EBV-positive B cells. For comparison purposes, the sequencing reads of this experiment and the previous ones were aligned to the NC\_007605.1 version of the EBV genome. From the comparison of CTCF tracks (Fig. 5), we observed minimal differences with respect to CTCF occupancy between latency types, except for the peaks at ~75 kb and ~122 kb that are predominantly present in gastric cancer and the peak at ~132 kb which is extremely variable between latency types.

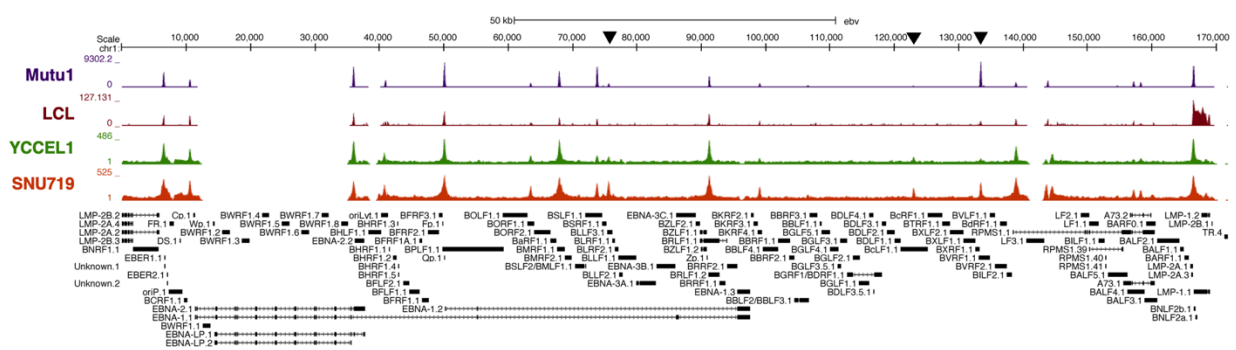


**Figure 5.** CTCF ChIP-seq profiles in latency Type I (Mutu, purple), III (LCL, brown) and II (YCCEL1, green and SNU719, dark red), normalized to input DNA. Arrowheads show the most different peaks between latency types.

To further confirm that the peaks observed in the ChIP-seq experiment were specific of CTCF, we conducted a binding motif analysis in both cell lines, which revealed that the recognized motifs correspond to CTCF and CTCFL (Fig. 6).

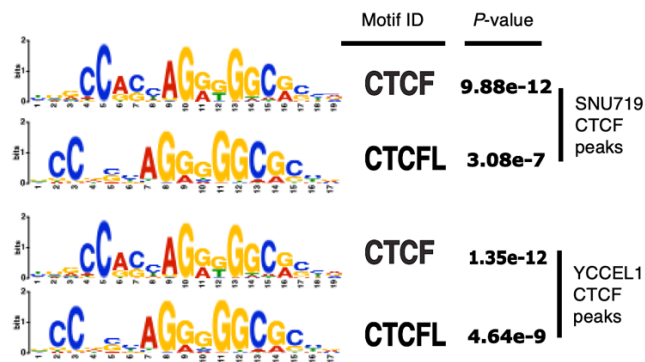


**Figure 6.** Motif analysis for the CTCF ChIP-seq peaks identified in the latency Type II cell lines.

Considering the established role of CTCF together with Cohesin complex in determining the formation of chromatin loops across the viral genome in B cells, we conducted a HiC experiment with the addition of an enrichment step for EBV-specific sequences (Figure 7), and identified the interactions present in the EBV genome in epithelial cells, and then compared them with those detected in EBV+ B cells.

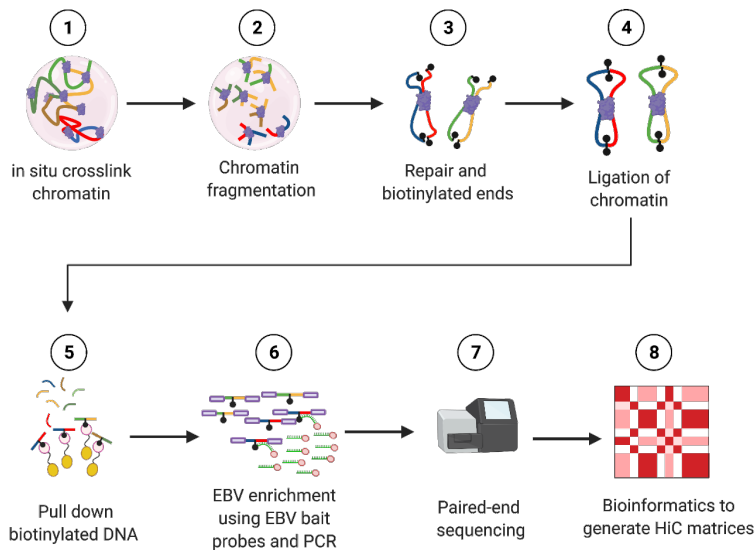


**Figure 7.** Schematic overview of the HiC assay with an added enrichment step for EBV. This step involves the use of biotin-tagged probes that hybridize to the EBV genome and are used to pull down EBV specific sequences.

Based on the Principal Component Analysis (PCA) of the 3D architecture of the viral genome (Fig. 8), EBV-infected cells were separated according to their tissue of origin. Both B cells and epithelial cells clustered separately based on the two main components, 1 and 2. Moreover, our analysis reveals that the episomes in the YCCEL1 cell line significantly differ from those in B cells, while the episomes in SNU719 show a conformation resembling more closely B-cell specific latencies.

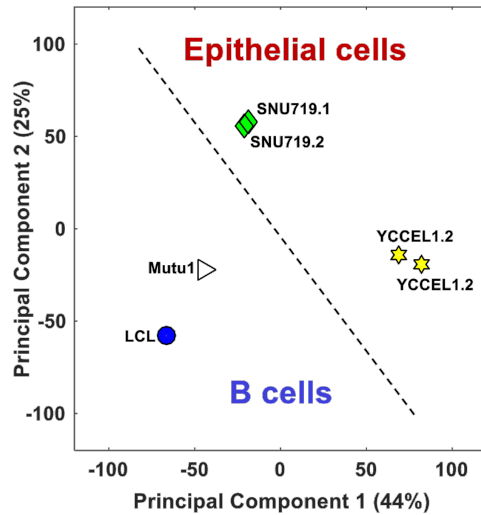


**Figure 8.** Principal Component Analysis (PCA) based on the 3D structure of the viral genome.

Next, the overall interactions were filtered based on CTCF binding and compared between B cells and GC cells. As shown in Figure 9, there are some interactions that occur more frequently in GC cells (in dark red in Fig. 9) that originate from the CTCF binding site on the LMP promoter (~166 kb) and terminate at the RPMS1 promoter region (~140 kb) or the Qp promoter (~50 kb), which is active in type II latency and transcribes for EBNA-1 gene. We observed that the number of interactions specific to B cells is higher compared to that of GC cells (in blue in Fig. 9). These specific interactions originate from three strong CTCF binding sites, namely the LMP promoter, the origin of replication Ori P (~6-8 kb), and the Cp promoter (~5-10 kb). Interestingly, the Cp promoter is active in B cells adopting the type III latency program and initiates the transcription for all the EBNAs.



inhibition period, we assessed the decrease in PARylation levels using Dot Blot (Figure 10).

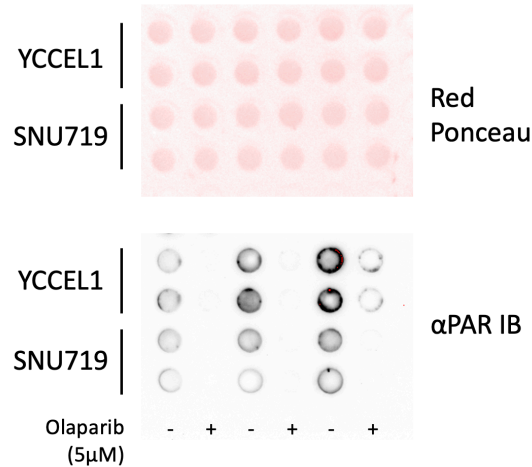


**Figure 10.** Red Ponceau staining (top) and Dot Blot (bottom) of poly (ADP-ribose) (PAR) in YCCEL1 and SNU719 cell lines upon PARP1 inhibition.

We then conducted a Chromatin Immunoprecipitation (ChIP) coupled with quantitative real-time PCR (qPCR) using antibodies against CTCF and the Cohesin subunit SMC1. In Type II EBV+ GC cells, our observations revealed a general trend of reduced CTCF binding, indicating that the absence of PARylation by PARP1 leads to the destabilization of binding at the viral genome level (Fig. 11A and 11B). This is consistent with our previous report that PARP1 activity is necessary to stabilize CTCF binding in B cells (Lupey-Green et al. 2018). However, only certain regions demonstrate a significant reduction in CTCF binding, such as the EBER promoter, the Qp promoter, the RPMS1 gene promoter, the lytic Zp promoter, and the LMP genes promoter. Interestingly, at the Cp promoter, which is silenced in latency type II cells, CTCF binding is unaffected by PARP1 inhibition (Fig. 11A and 11B), in contrast to what we observed in type III latency (Lupey-Green et al. 2018).

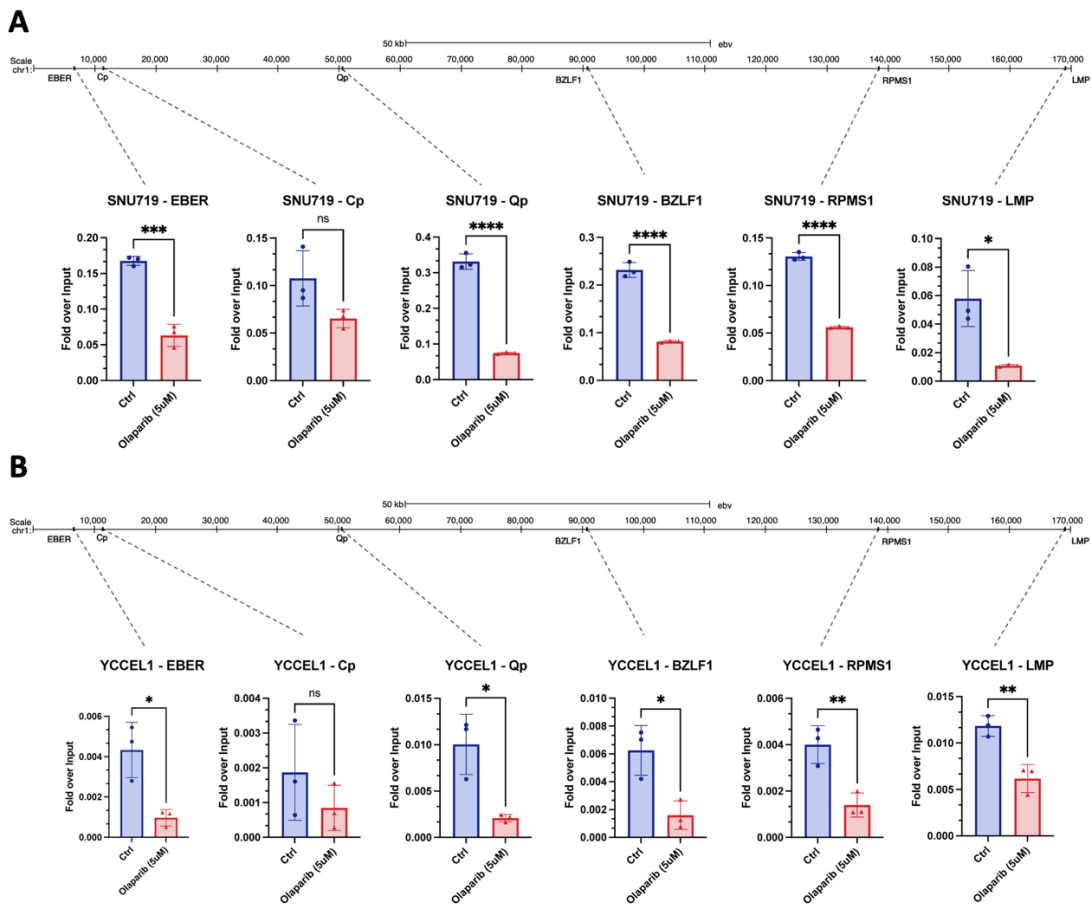


**Figure 11. A** CTCF ChIP-qPCR in SNU719 cell line following PARP1 inhibition with 5uM Olaparib treatment for the main CTFC binding sites. **B** CTFC ChIP-qPCR in YCCEL1 cell line following PARP1 inhibition with 5uM Olaparib treatment for the main CTFC binding sites. Data are presented as %input. N = 3, Mean  $\pm$  SD. The t test p values for the Olaparib/Ctrl comparison are indicated as asterisks (\*\*\*\* =  $p \leq 0.0001$ , \*\*\* =  $p \leq 0.001$ , \*\* =  $p \leq 0.01$ , \* =  $p \leq 0.05$ ).

These results suggest that although PARP1 activity generally regulates CTFC binding across the entire EBV genome, the specific EBV regions that experience a loss of CTFC binding after PARP inhibition are dependent on the cell type and latency type. In other words, the impact of PARP inhibition on CTFC binding is context-specific and varies based on the characteristics of the infected cell and the type of latency exhibited by EBV.

Due to the close correlation observed between CTCF and Cohesin binding across the EBV genome in B cells, we assessed further the SMC1 binding at the same regions analyzed for CTCF. Surprisingly, in contrast to what observed in Type III B cells, Cohesin subunit binding shows random alterations at all the analyzed regions (Fig. 12A and 12B) when PARP1 is inhibited. This suggests a potential destabilization of Cohesin binding induced by the inhibition of PARP1 activity.

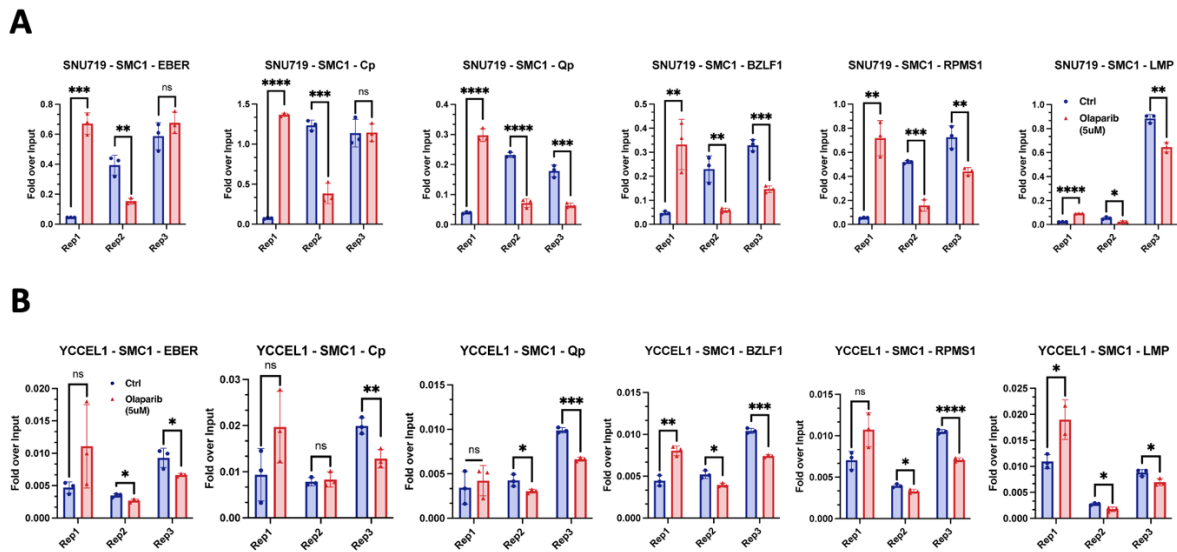


**Figure 12. A** ChIP-qPCR in SNU719 cell line following PARP1 inhibition for SMC1 Cohesin subunit in all three replicates for the same CTCF binding sites. **B** ChIP-qPCR in YCCEL1 cell line following PARP1 inhibition for SMC1 Cohesin subunit in all three replicates for the same CTCF binding sites. Data are presented as %input. N = 3, Mean  $\pm$  SD. The t test p values for the Olaparib/Ctrl comparison are indicated as asterisks (\*\*\*\* =  $p \leq 0.0001$ , \*\*\* =  $p \leq 0.001$ , \*\* =  $p \leq 0.01$ , \* =  $p \leq 0.05$ ).

Considering the observed differences in CTCF and SMC1 binding across the EBV genome after PARP inhibition, and their role in promoting long-range chromatin loops (Rao et al. 2014; K. Zhang et al. 2016), we next determined whether there were changes in the viral genome architecture. To do this, we performed a Hi-C experiment in both cell lines following a 72-hour treatment with Olaparib. Similar to the observed alterations in B cells, EBV+ GC cells also undergo changes in the 3D structure of the EBV episomes

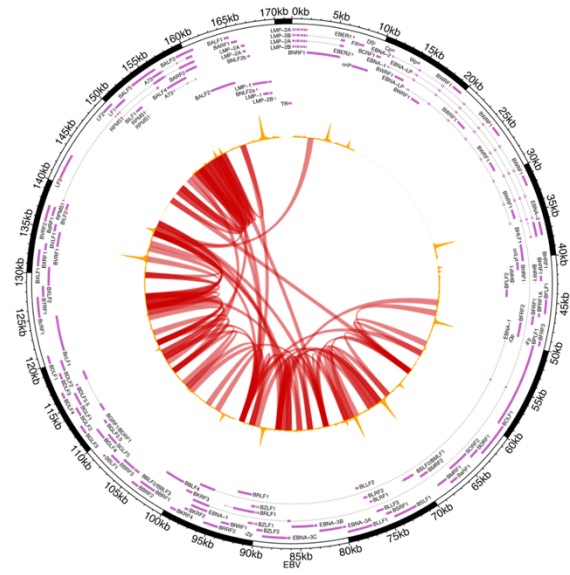
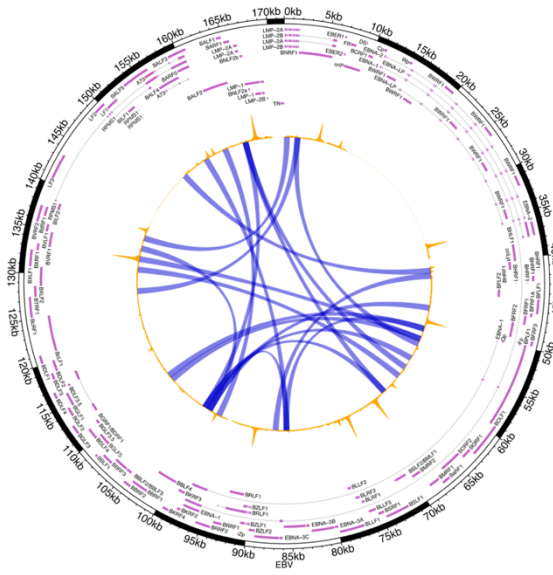
upon PARP1 inhibition. These changes include a reduction in the length of interactions, indicating that loops occur more frequently between adjacent regions. However, certain long-range interactions originating from the LMP1 gene promoter region remain unaffected and unchanged (Fig. 13). Notably, the YCCEL1 cell line is more profoundly affected by PARP1 inhibition, displaying a significant decrease in the length of interactions and a shift in the origin of long-range loops, that now originate from the CTCF peak at the LMP gene promoter instead of the LMP2A/B gene region (Fig. 13B).

**A**

**EBV – SNU719**

**Control**

**Olaparib**



**B**

**EBV – YCCEL1**

**Control**

**Olaparib**

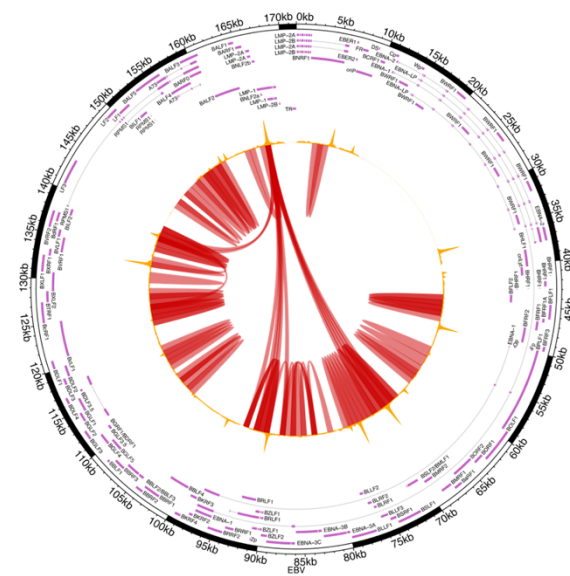
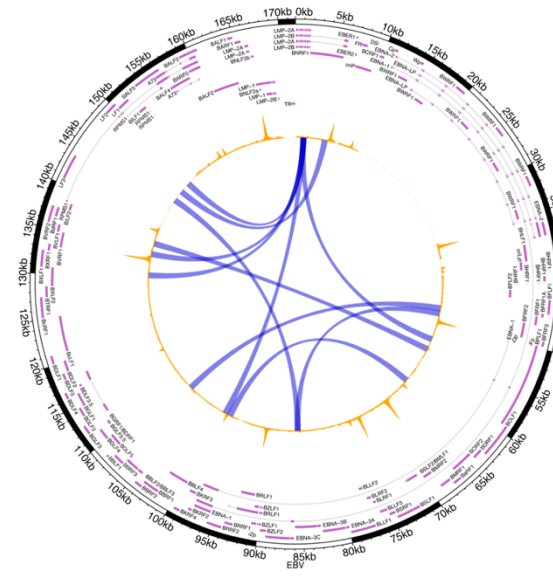


**Figure 13. A** Circular visualization of the interactions derived from HiC matrices in SNU719 cell line. The arches represent the DNA-DNA interactions at 1 kb scale. The blue arches represent the interactions found more frequently in the control samples, while the red ones represent those found more frequently in the Olaparib treated samples (FDR < 5%). **B** Circular visualization (as described in A) of the interactions derived from HiC matrices in YCCEL1 cell line. In all plots CTCF ChIP-seq track is represented in yellow on top of the arches.

Overall, the results indicate that the inhibition of PARP1 has a significant impact on CTCF and Cohesin binding not only in B cells but also in EBV+ gastric cancer cells. This disruption in the binding of these architectural proteins leads to alterations in the 3D structure of the viral genome. The changes observed in the interactions and loops within the viral episomes are likely to play a crucial role in regulating viral gene expression and may have implications for the development and progression of gastric cancer associated with EBV infection. These findings highlight the importance of PARP1 activity in maintaining the proper architecture and function of the EBV genome in different cell types and latency types.

### **3.3 PARPi affects viral gene expression**

To determine whether the variations in CTCF and Cohesin binding observed after PARP1 inhibition were generalized throughout the host genome or specific to EBV episome, we performed subcellular fractionation and analyzed by Western Blot Cohesin subunits, CTCF and PARP1 for their presence in the chromatin-associated protein fraction (Fig. 14) in both cell lines. We observed that after PARP1 inhibition the YCCEL1 cells exhibit a noticeable increase in the chromatin-associated fraction of Cohesin subunits SMC3, SMC1A, and RAD21 (Fig. 14A), with statistical significance observed for SMC1A and RAD21 (Fig. 14B). However, the fractions of CTCF and PARP1 in YCCEL1 cells remain unchanged. Conversely, the SNU719 cell line displays consistent levels of chromatin-bound proteins without any notable variation (Figs 14A and 14B).

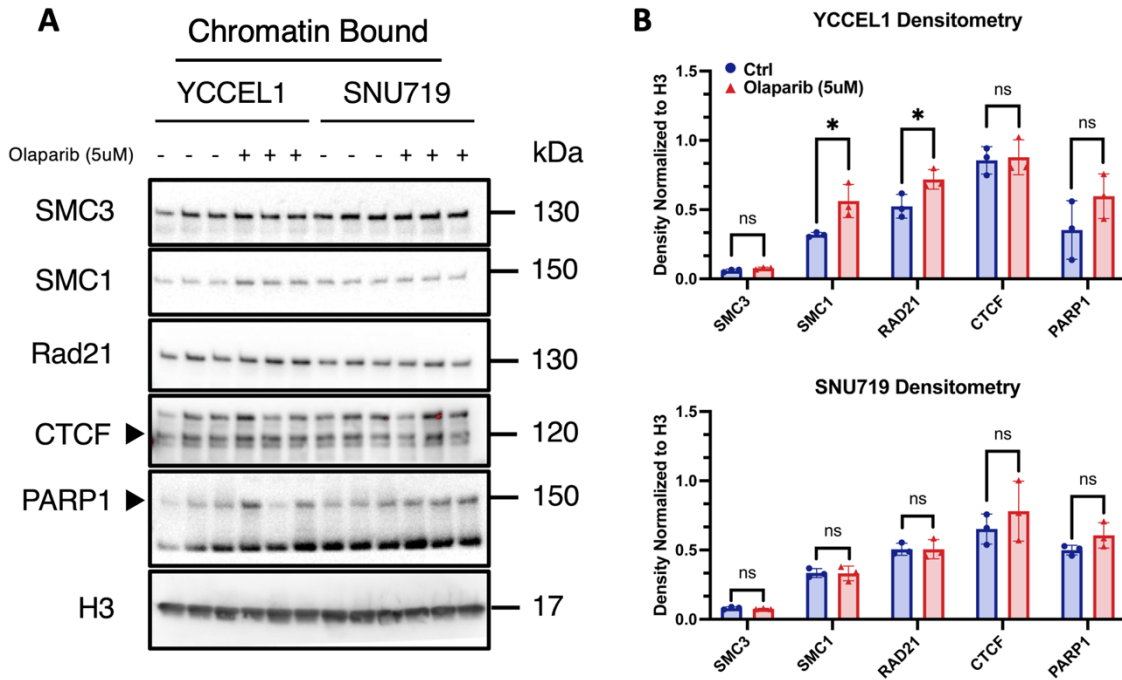


**Figure 14. A** Western Blot of chromatin-bound fraction of Cohesin subunits, CTCF and PARP1 proteins extracted from YCCEL1 and SNU719 cell lines following PARP1 inhibition (N = 3). Molecular weights are indicated on the side. **B** Densitometry analysis of the western blot described in A. Data are normalized on the H3 histone density. The t test p values for the Olaparib/Ctrl comparison are indicated as asterisks (\* =  $p \leq 0.05$ ).

To determine whether the differences observed in subcellular fractionation were linked to a widespread increase in the expression of genes encoding Cohesin subunits, we performed Reverse Transcription quantitative Real-Time PCR (RT-qPCR). However, in both cell lines, we did not find any significant increase in the expression of Cohesin subunits and CTCF, as illustrated in Figure 15.

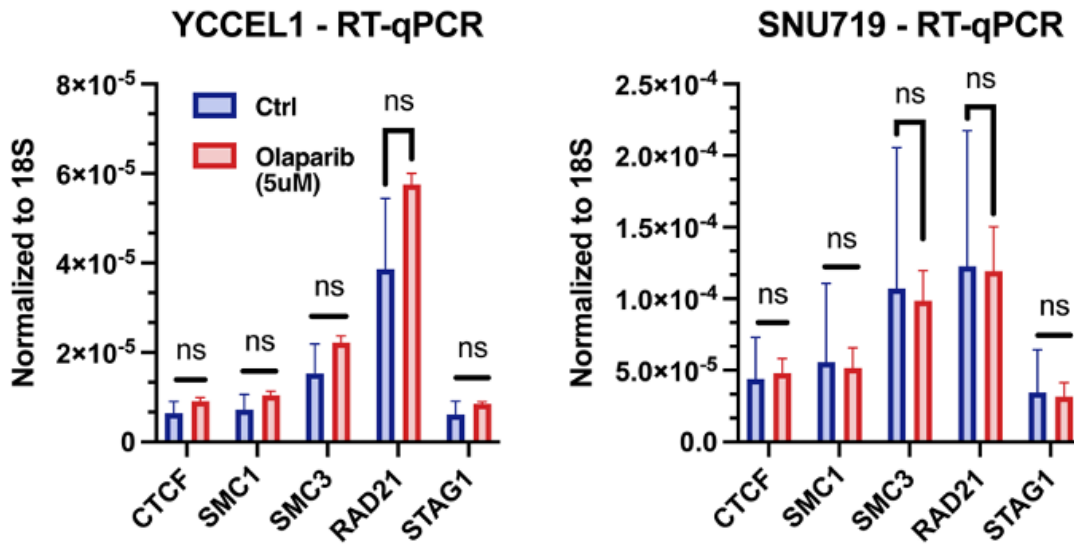


**Figure 15.** RT-qPCR in YCCEL1 (left) and SNU719 (right) for CTCF and all the components of the Cohesin complex following Olaparib treatment. N = 3, Mean ± SD.

We recently have shown that alterations in CTCF and Cohesin binding, along with changes in the 3D architecture of the EBV genome, have significant effects on viral gene expression in B cells (Morgan et al. 2022). These observations suggest a potential link between chromatin organization and viral gene regulation in infected cells. To gain further insights into the connection between chromatin organization and the regulation of viral genes within epithelial infected cells, we conducted RT-qPCR analysis focusing on specific latent genes expressed in Type II latency, including EBNA-1 and LMP2, along with the viral DNA polymerase processivity factor BMRF1, expressed in the early phases of the lytic cycle. By examining the expression levels of these genes, we aimed to gain a comprehensive understanding of the impact of chromatin organization on the transcriptional regulation of key EBV genes during Type II latency. Our analysis revealed intriguing findings regarding the YCCEL1 and SNU719 cell lines in response to Olaparib treatment. In the YCCEL1 cell line, we observed a significant increase in the expression of the BMRF1 gene, while the expression of the two analyzed latent genes, EBNA-1 and

LMP2, remained unchanged. In the SNU719 cell line, there was a non-significant change in the expression of the three genes analyzed (Figure 16).

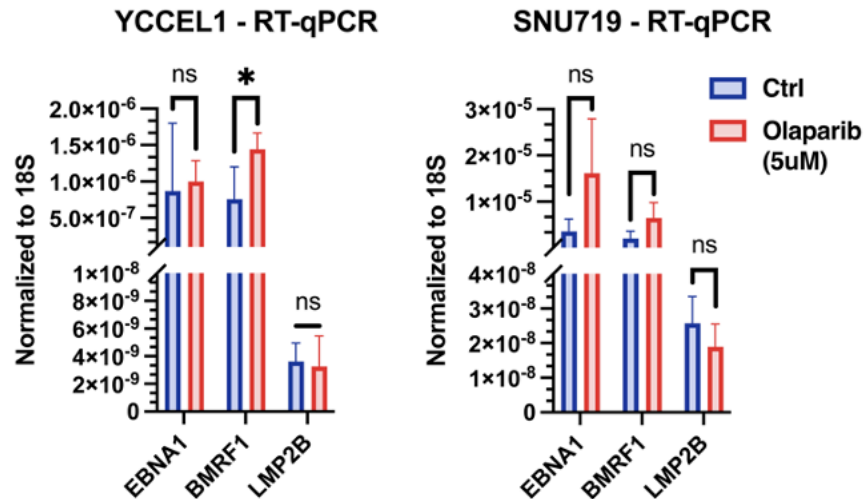


**Figure 16.** RT-qPCR of EBNA-1, BMRF1 and LMP2B viral genes following Olaparib treatment. Bar graph represents the average expression of three biological replicates per treatment, each normalized to 18S expression, respectively. ( $N=3$ , mean  $\pm$  SD). Paired student's  $t$  test assuming equal variance (two-tailed) was used to compare the experiments ( $* = p \leq 0.05$ ).

Moreover, the small differences observed in gene expression could be attributable to different activity of PARP1 between latency types. These results mirror the findings in Mutu1 cell line harboring a Type I latency (Morgan et al. 2022). In this cell line characterized by low basal levels of PARylation, treatment with a PARP inhibitor resulted in significant changes in the expression of only three viral genes (Morgan et al. 2022). In the Gastric Carcinoma cell lines, we observed a substantial disparity in PAR levels compared to Lymphoblastoid Cell Lines (LCLs) which appeared to be the most responsive to PARP1 inhibition, leading to dysregulation in latent viral gene expression. To quantify intracellular PAR levels, we conducted a PAR ELISA (Figure 17). Given the diminished activity of PARP1 in these cells, it is not surprising to observe minimal differences in gene expression following PARP1 inhibition. Furthermore, the variance in

PAR levels between YCCEL1 and SNU719 cells may explain the notable disparity in BMRF1 expression.

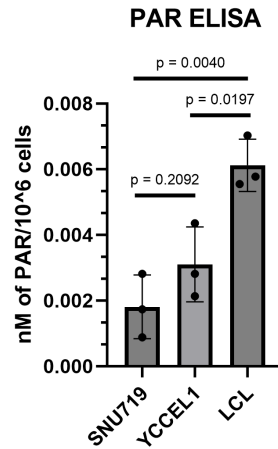


**Figure 17.** ELISA assay conducted on SNU719, YCCEL1 and LCL cell lines. N = 3, Mean ± SD. The t test p values are indicated above.

Remarkably, despite the increased expression of BMRF1 in YCCEL1 cell line, the overall copy number of EBV within the cells treated with Olaparib remained unaltered, as shown in Figure 18. This suggests that Olaparib treatment led to the destabilization of the viral genome, leading to unrestricted expression of viral latent and lytic genes without causing an increase in the viral copy number.

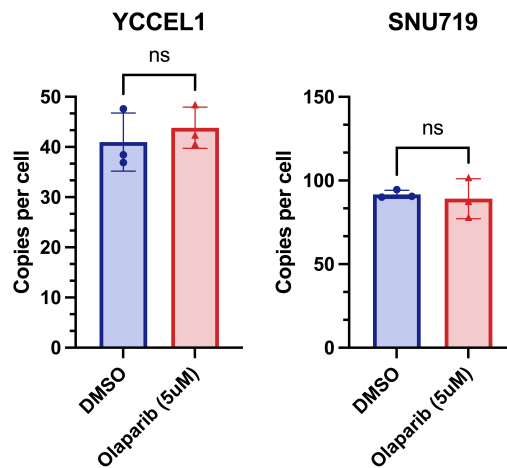


**Figure 18.** Droplet Digital PCR (ddPCR) assessing the viral copy number in YCCEL1 and SNU719 cell lines upon Olaparib treatment.

These findings provide valuable insights into the mechanisms underlying Olaparib impact on EBV-infected cells, shedding light on the complex interplay between chromatin organization, viral gene expression, and viral genome stability.

### 3.4 CTCF occupies viral regions with an enhancer epigenetic signature

In our recent study, we have delved into the three-dimensional structure of the viral genome in two different latency types of EBV and presented experimental evidence that underscores the strong correlation between the architecture of episomes and viral gene expression (Morgan et al. 2022). Moreover, recent research (Ding et al. 2022), has indicated the presence of viral genomic regions enriched with histone marks typical of enhancers, such as H3K4me1 and H3K27ac. To further understand the functional implications of the observed genomic architecture of EBV in these two cell lines, we conducted a ChIP-seq experiment using antibodies targeting H3K4me1 and H3K27ac. These histone marks are known to respectively indicate poised and active enhancers. Our analysis revealed a notable enrichment of these two histone marks at specific regions of the viral genome, particularly at the origins of replication OriP and OriLyt, as well as the promoters Qp, Zp, BILF2, and LMP genes (Fig. 19).

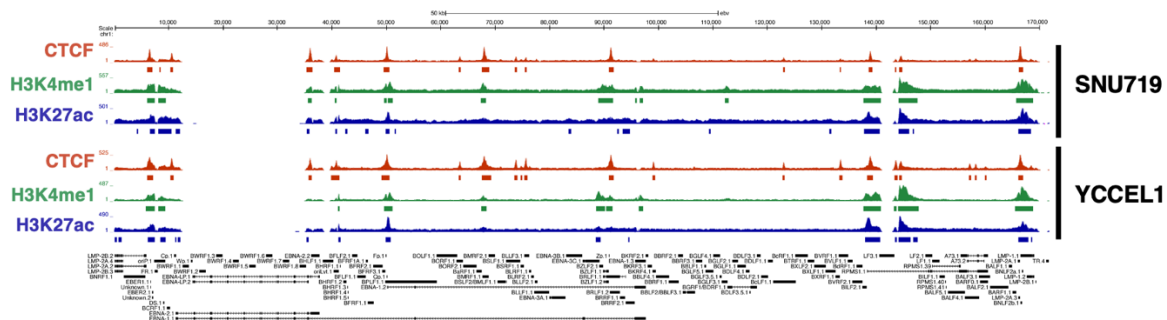


**Figure 19.** UCSC Genome Browser tracks for CTCF (dark red), H3K4me1 (green), H3K27ac (blue) on the EBV genome in both SNU719 (top) and YCCEL1 (bottom) cell lines.

These findings provide compelling evidence that the genomic organization of EBV in these cell lines indeed serves a functional purpose, specifically in regulating viral gene expression through enhancer activity. Based on the location of the peaks for both histone modifications, we conducted a transcription factor binding motif analysis (Fig. 20). In both GC cell lines, the peaks of H3K4me1 were consistently associated with CTCF binding motifs. This suggests that CTCF may play a significant role in the regulatory activity of these enhancers in both cell lines. However, the peaks of H3K27ac exhibited greater variability between the two cell lines. In the SNU719 cell line, the most frequent binding motifs were identified as ZBT17 and ZEB1. This indicates that these transcription factors might be crucial for the enhancer activity and gene regulation specific to this cell line. In contrast, the YCCEL1 cell line showed predominant binding motifs for CTCF and EGR1 at the peaks of H3K27ac. This suggests a different transcription factor landscape in this cell line, possibly contributing to distinct enhancer activities and gene expression patterns.

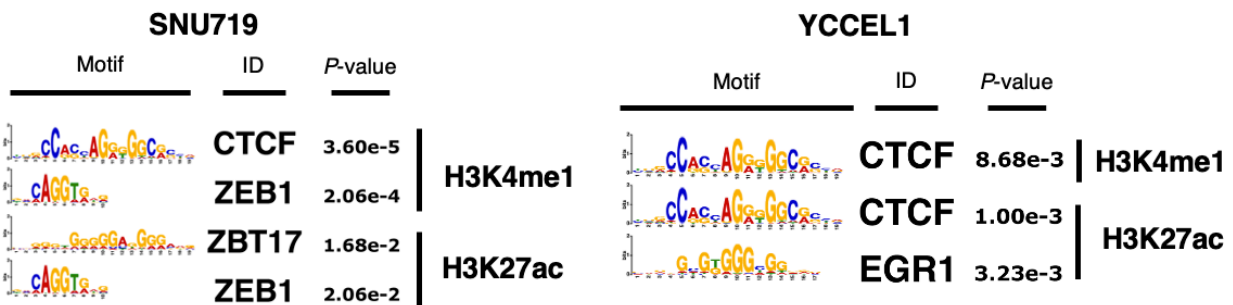


**Figure 20.** Transcription factor motif analysis for H3K4me1 (top) and H3K27ac (bottom) peaks in SNU719 (left) and YCCEL1 (right) cell lines.

These findings indicate that the regulatory landscape of enhancers, marked by H3K4me1 and H3K27ac, varies between the two cell lines, and specific transcription factors may be pivotal in mediating the enhancer activity and subsequent gene expression profiles.

Next, we conducted an overlap analysis between CTCF peaks and the peaks associated with the enhancer chromatin signature. Analysis of CTCF, H3K4me1, and H3K27ac peaks (Fig. 21) revealed substantial overlap, with 8 peaks in SNU719 and 7 in YCCEL1, while the number of unique CTCF peaks was notably higher in YCCEL1, being twice that

of SNU719. Notably, a shared region at the BMRF1 promoter in both cell lines exhibited only CTCF and H3K4me1, indicating a poised enhancer region.

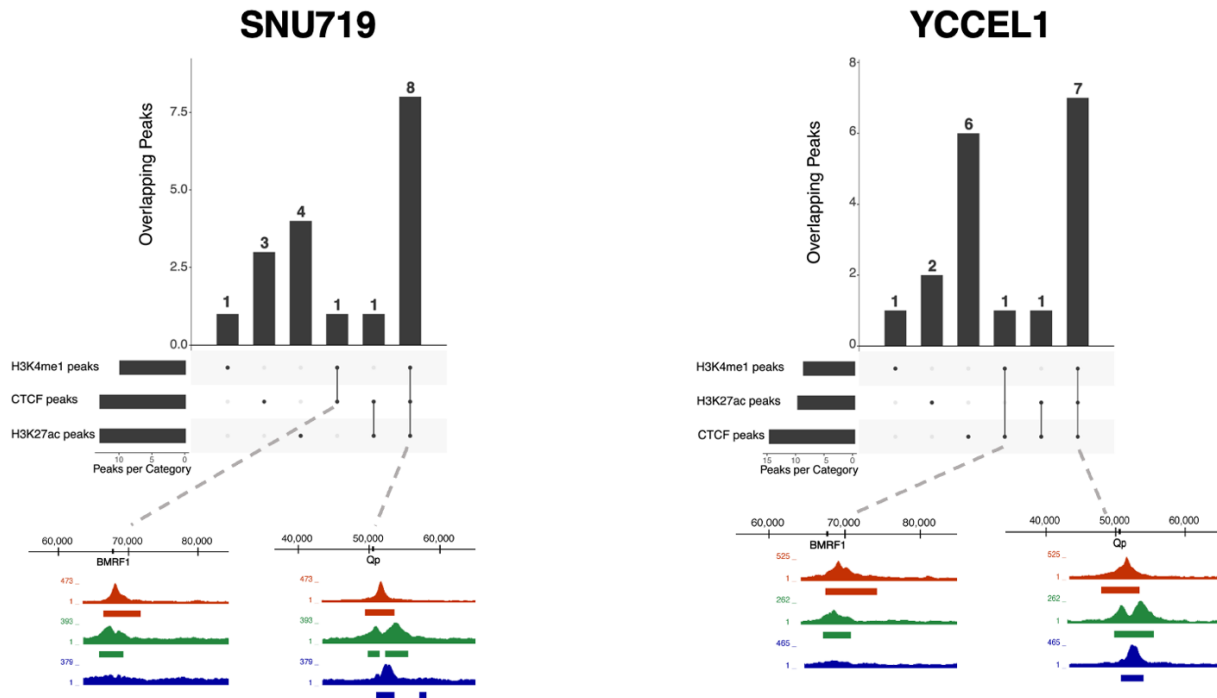


**Figure 21.** UpSet plot of the overlap between CTCF and H3K4me1 and H3K27ac histone marks. On the bottom, magnified ChIP-seq tracks for CTCF and both histone marks are shown.

Comparing H3K4me1 and H3K27ac peaks between LCL and GC cell lines (Fig. 22), both histone marks showed fewer peaks in LCL compared to GC cells. These modifications were prominently enriched at the Cp promoter but completely absent at the Qp promoter, aligning with the distinct activities of these promoters in different latency types.

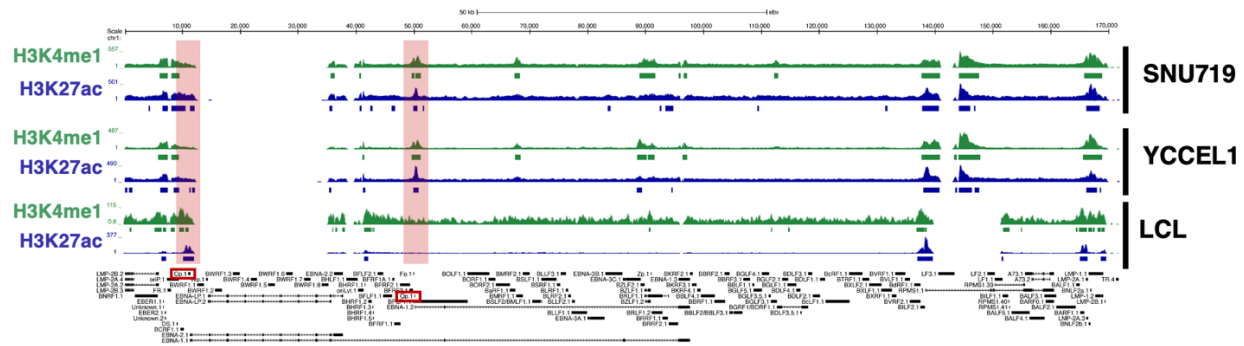


**Figure 22.** H3K4me1 and H3K27ac ChIP-seq tracks on the EBV genome in SNU719 (top), YCCEL1 (middle) and LCL (bottom) cell lines.

These findings suggest functional relevance of the 3D structure of the EBV genome, bringing active enhancers into close proximity. CTCF, along with other transcription factors, likely plays a crucial role in mediating these processes across the EBV genome. This highlights the importance of chromatin organization and histone modifications in controlling EBV gene expression and may offer valuable insights into the mechanisms underlying EBV-associated diseases.

### 3.5 HiChIP analysis reveals distinct three-dimensional structures and enhancer interactions in SNU719 and YCCEL1 cell lines

To further strengthen the correlation between the three-dimensional structure and regions characterized by enhancer marks across the EBV genome, we conducted a HiChIP experiment for the H3K27ac histone modification. In HiChIP assay, long-range DNA interactions are first established *in situ* in the nucleus before lysis, minimizing possible false-positive interactions. Then ChIP is performed on the contact library, thus capturing long-range interactions associated with a protein of interest. Paired-end sequencing is used to identify two distantly located segments of the genome from one fragment, indicating that the factor of interest was associated with the long-range interaction (Mumbach et al. 2016) (Figure 23).

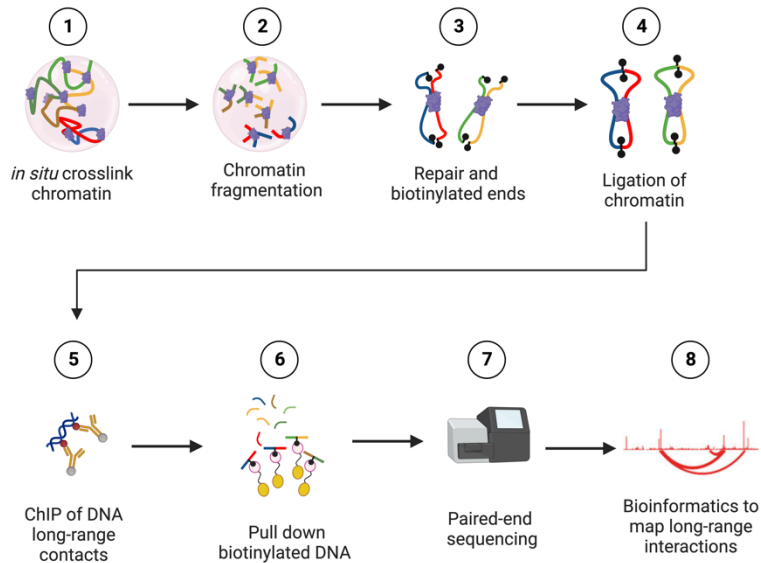


**Figure 23.** Schematic overview of the HiChIP assay.

The Principal Component Analysis (Fig. 24), indicates distinct clustering of the two cell lines, suggesting that the interactions between regions enriched for the H3K27ac histone mark vary between them.

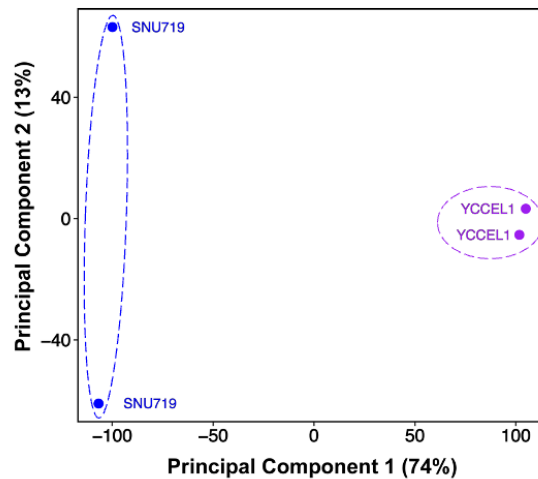


**Figure 24.** Principal Component Analysis (PCA) of H3K27ac HiChIP.

Building on this observation, we conducted a differential analysis of interactions occurring between different regions of the viral genome to explore how H3K27ac-enriched

chromatin loop vary between the two cell lines. We observed that the SNU719 cell line exhibits a higher number of interactions that occur more frequently compared to the YCCEL1 cell line (Fig. 25). Conversely, the YCCEL1 cell line presents only three frequent interactions, specifically between the promoter regions of the LMP2A/B genes and the promoter of LMP1, as well as interactions involving the BILF2 region, and between the promoters of LMP1 and Zp (Fig. 25). However, both cell lines share a common interaction between the LMP promoter and a region enriched with H3K27ac, located approximately 20 kb upstream the promoter (Fig. 25). This interaction appears to be conserved between the two cell lines despite their distinct characteristics, further supporting the significance of this interaction in the regulation of viral gene expression.

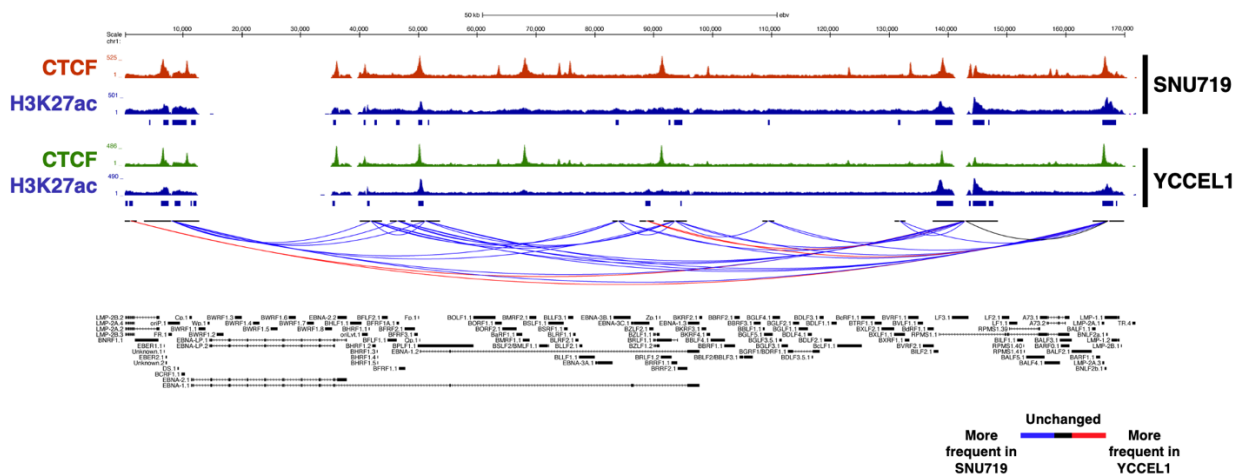


**Figure 25.** UCSC Genome Browser tracks of CTCF (dark red and green) and H3K27ac (blue) on the EBV genome in SNU719 (top) and YCCEL1 (bottom) cell lines. On the bottom of the image are show the unique H3K27ac-rich interactions (FDR < 1%) in both cell lines (blue = more frequent in SNU719, red = more frequent in YCCEL1, black = no difference in frequency between cell lines).

### 3.6 EBV enhancer regions are tethered to specific loci across the host genome

In previous studies utilizing HiC or 4C assays, it was revealed that the EBV genome is connected to the host genome, suggesting a potential role in regulating host gene expression in infected cells (K.-D. Kim et al. 2020; Okabe et al. 2020). To further

investigate this phenomenon, we delved into the possibility of specific physical connections between the identified viral enhancer regions and particular loci within the host genome. To achieve this, we analyzed H3K27ac HiChIP datasets for chromatin loops formed between viral and host genomic regions.

Through the HiChIP experiment, we were able to detect around 70 interactions taking place between the EBV genome and the human genome across both cell lines. To focus specifically on robust EBV-human interactions, we considered loops with more than 3 reads and visualized them in circos plots. In these plots, the EBV genome was represented in red and positioned at the top (see Fig. 26A/B). This visualization allowed us to highlight the significant interactions between EBV and the human genome for further analysis and interpretation.

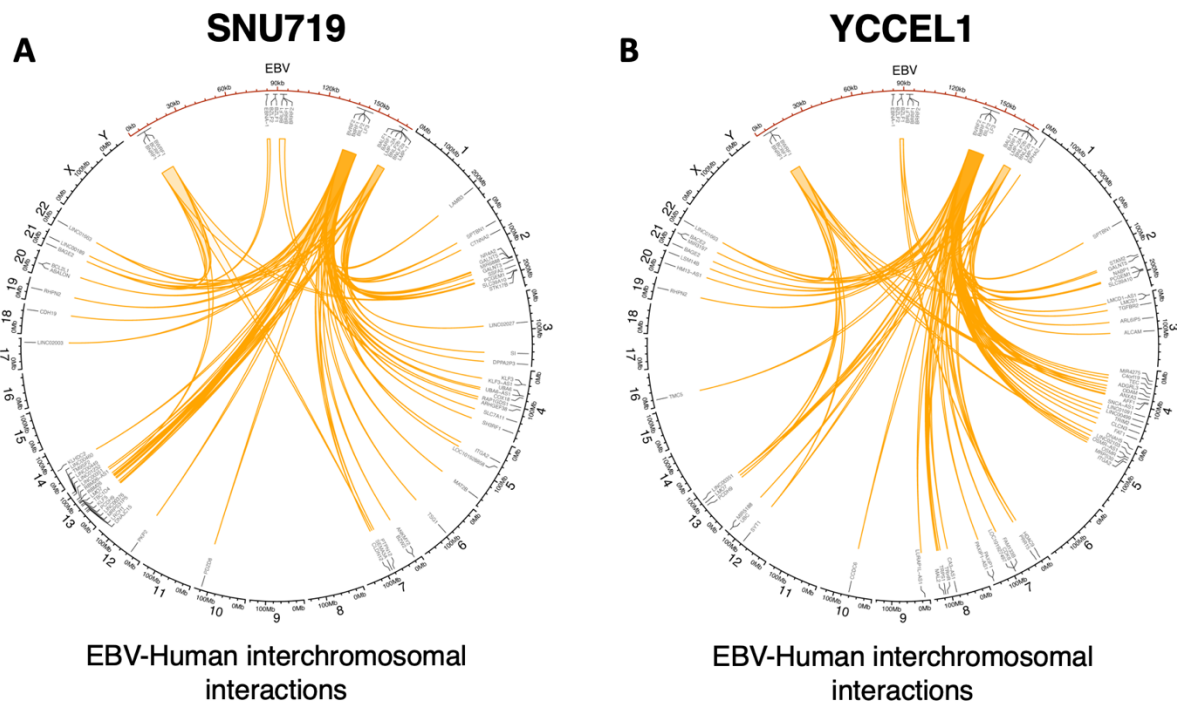


**Figure 26. A** Circos plot of EBV-Human interchromosomal interactions for SNU719 cell line. EBV is represented in red and enlarged on the top section of the plot. EBV-Human interactions are represented as orange arches. Some of the genes near the interaction points are annotated. **B** Circos plot of EBV-Human interchromosomal interactions for YCCEL1 cell line (as described in A).

An important observation we made was that, in contrast to recent studies conducted by Japanese researchers (Okabe et al. 2020), most of the interactions we identified did not originate from the OriP region of the EBV genome (Fig. 27). Instead, they predominantly arose from the BILF2 and LMP regions. This finding suggests that these two regions likely act as strong enhancers, a characteristic that had been previously highlighted by other research groups, particularly concerning Type II latency in B cells (Ding et al. 2022).

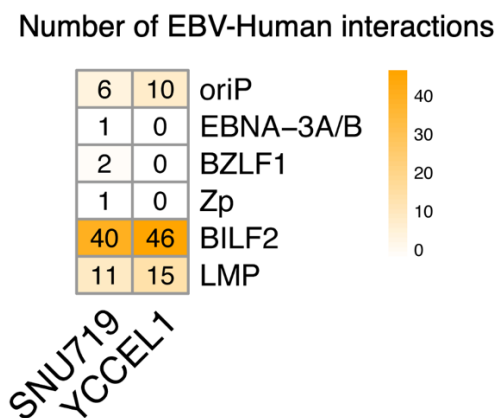


**Figure 27.** Heatmap highlighting the regions of the EBV genome involved in EBV-Human interactions.

Furthermore, despite the involvement of the same regions of the EBV genome in the chromatin loops, the corresponding regions of the human genome differed between the two GC cell lines (SNU719 and YCCEL1). Notably, in the SNU719 cell line, chromosomes 2, 4, 13, and 21 exhibited the highest number of interactions with the EBV genome. In contrast, the YCCEL1 cell line displayed the highest number of interactions with chromosomes 2, 4, 5, 7, and 13 (Fig. 28A).

Moreover, we analyzed the transcription factor binding motifs present at this EBV docking sites (Figure 28B). Interestingly, the top 5 motifs identified were similar between the two cell lines, suggesting a possible key role for these transcription factor in the maintenance of these EBV-Human interactions.

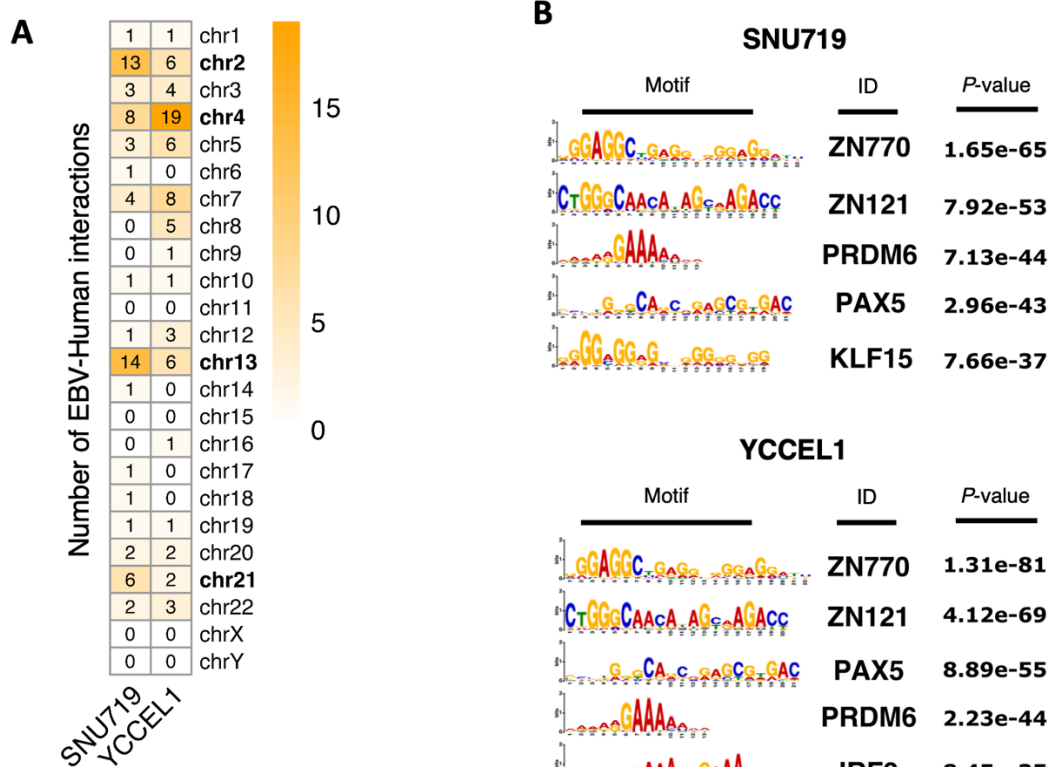


**Figure 28. A** Heatmap showing the number of interactions occurring between EBV and the Human chromosomes in both cell lines. **B** Transcription factor motif analysis of EBV-Human interaction regions on the Human genome for SNU719 (top) and YCCEL1 (bottom) cell lines.

Furthermore, there are differences in the number of interactions originating from the three EBV enhancer regions. By comparing the loops occurring between EBV and the Human chromosomes 2 and 13, which are common between the two cell lines, we observed that the SNU719 cell line exhibits more frequent interactions originating from BILF2 and LMP enhancer regions respect to the YCCEL1 cell line. On the other end YCCEL1 cell line shows more frequent interactions between BILF2, LMP and oriP and chromosome 4 (Fig. 29).

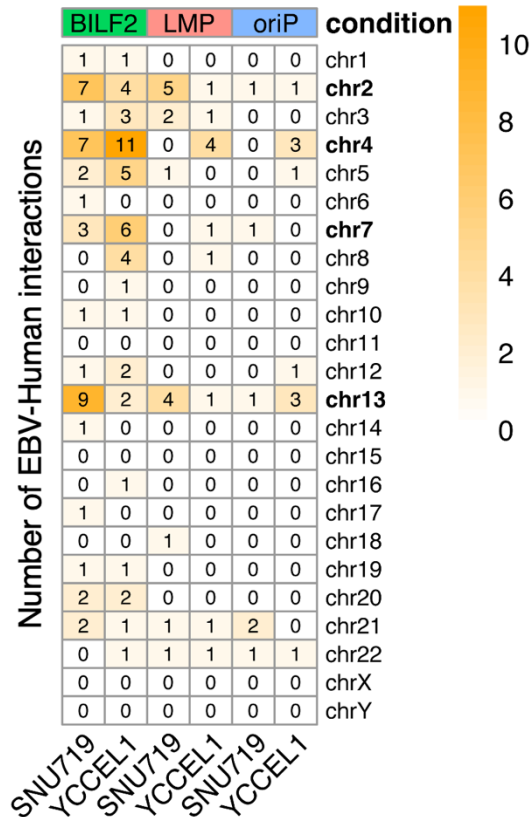


**Figure 29.** Heatmap showing the number of EBV-Human interchromosomal interactions classified based on the regions of the EBV genome involved (green, red and cyan) and the cell line.

These distinctions in the human genome regions involved in interactions suggest cell line-specific differences in the regulatory mechanisms and potential implications for EBV-host interactions in the context of these two cell lines.

Indeed, the data obtained from the HiChIP experiment strongly indicate that the two cell lines (SNU719 and YCCEL1) not only exhibit differences in the 3D structure of the EBV genome but also in the specific interactions that take place between the EBV episomes and the Human genome. By forming such interactions, EBV enhancers can exert their regulatory effects on host genes, modulating their expression and influencing various cellular processes.

### 3.7 Functional Role of EBV-Human Interactions: Gene Expression Analysis Reveals Strong Viral Enhancers Associated with Gastric Cancers

To determine if the interactions between EBV enhancer and the Human genome had functional significance, we evaluated the expression of cellular genes in proximity to the viral interaction sites. To achieve this, we focused on H3K27ac-mediated loops which were filtered based on the approximately 70 viral-human looping sites previously identified and examined only the genes whose Transcription Start Site (TSS) fell within a 1 kb region from the H3K27ac peak considered. This approach allowed us to pinpoint genes that were in close proximity to the regions of active chromatin marked by H3K27ac and that might potentially be influenced by the EBV enhancers.

In the YCCEL1 cell line, approximately 300 genes were identified near the EBV-human interaction sites, while in SNU719, around 200 genes were identified (as shown in Fig. 30). Interestingly, only 53 of these genes were found to be common between the two cell lines, indicating a considerable degree of cell line-specificity in the genes influenced by the EBV enhancers.

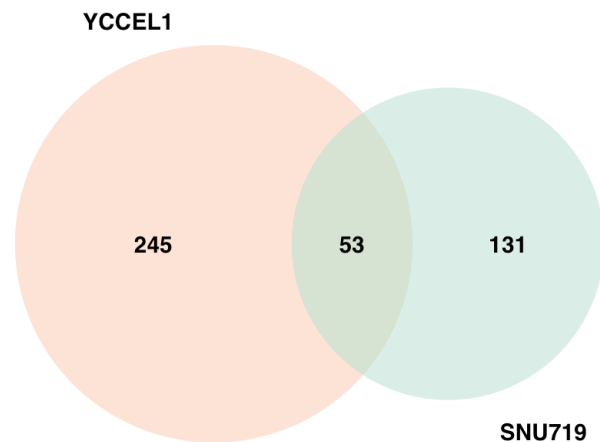


**Figure 30.** Venn Diagram showing the overlap between the genes found near the EBV-Human interaction regions in YCCEL1 and SNU719 cell lines.

To further investigate the functional impact of these interactions, we analyzed the expression levels of these identified genes using RNA sequencing (RNA-seq) data obtained from the SNU719 cell line (as depicted in Fig. 31A). Comparing the expression levels of these genes to two sets of randomly selected genes, we observed that the genes located near the EBV interaction sites displayed significantly higher expression levels. This difference in expression between the genes near EBV interaction sites and the randomly selected genes was found to be statistically significant, underscoring the potential regulatory role of the EBV enhancers in influencing the expression of nearby host genes.

To investigate whether similar gene expression patterns were present in patients with EBV-positive gastric tumors, we examined the expression of the two sets of genes identified in the cell lines, along with three sets of random genes, using The Cancer Genome Atlas (TCGA) database. Once again, we observed that all the genes located near the EBV-Human interactions exhibited significantly higher expression levels (as depicted in Fig. 31B/C).

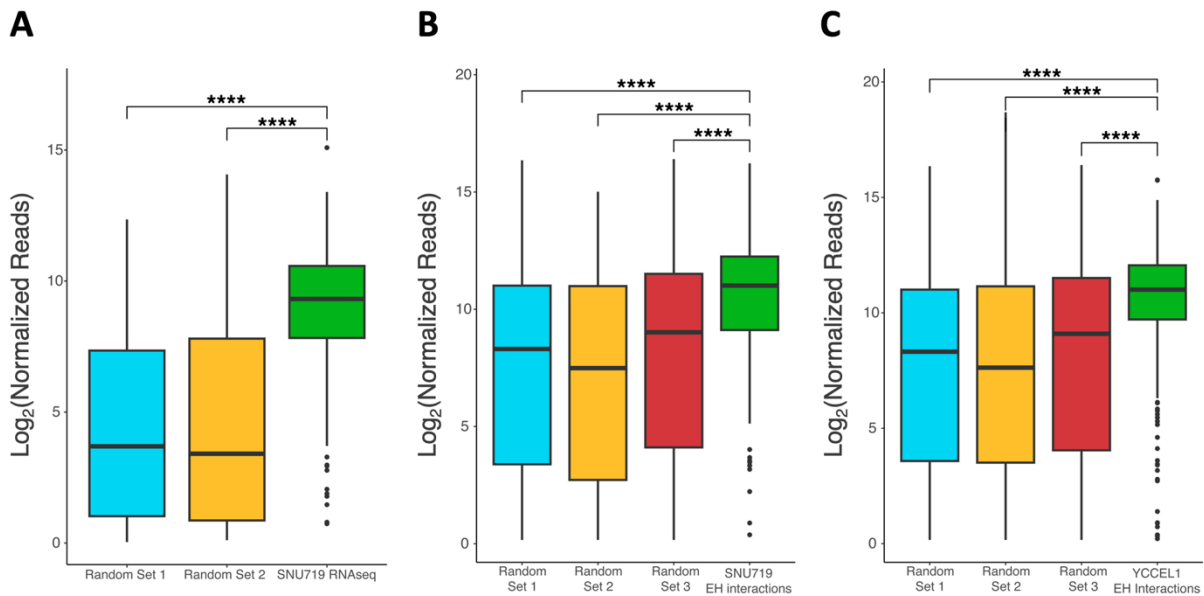


**Figure 31.** **A** Boxplot comparing the normalized reads for genes near EBV-Human interactions to two different random gene sets in SNU719 cell line (\*\*\*\* =  $p \leq 0.0001$ ). **B** Boxplot comparing the normalized reads for genes near EBV-Human interactions found in SNU719 to three different random gene sets in TCGA datasets from biopsies of EBV+

gastric malignances (\*\*\*\* =  $p \leq 0.0001$ ). **C** Boxplot (as described in B) for EBV-Human interactions found in YCCEL1 cell line (\*\*\*\* =  $p \leq 0.0001$ ).

To further assess if the overexpression of these genes was correlated to the presence of EBV episomes in proximity to those regions we conducted a bioinformatic analysis on publicly available RNA-seq datasets from Okabe et al. (Okabe et al. 2020). In particular, we reanalyzed the RNA-seq experiments conducted on normal gastric epithelial cells (GES) before and after EBV infection. Similarly to what we observed in SNU719, the genes near EBV tethering regions appeared significantly upregulated upon EBV infection respect to the wildtype condition (Figure 32).

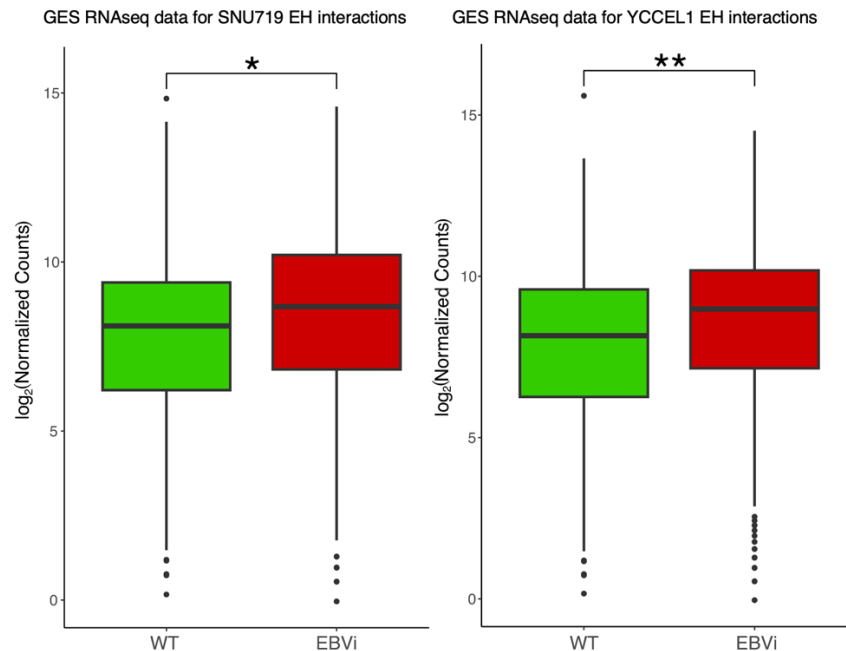


**Figure 32.** Boxplot of the normalized reads for genes near EBV-Human interactions for SNU719 cell line (left) and YCCEL1 cell line (right) between normal gastric epithelial cells (GES) before (WT) and after EBV infection (EBVi) (Wilcoxon t test, \*\* =  $p \leq 0.01$ , \* =  $p \leq 0.05$ ).

Subsequently, to explore the potential role of these genes in the neoplastic transformation of EBV-infected cells, we performed an Ingenuity Pathway Analysis (IPA) focusing on the

genes located near the viral genome in both cell line (Fig. 33A/B). The analysis of Disease and Functions associated with these genes revealed prominent associations with "Cancer" and "Gastrointestinal Disease", implying that these genes may serve as crucial markers of gastric cancers.

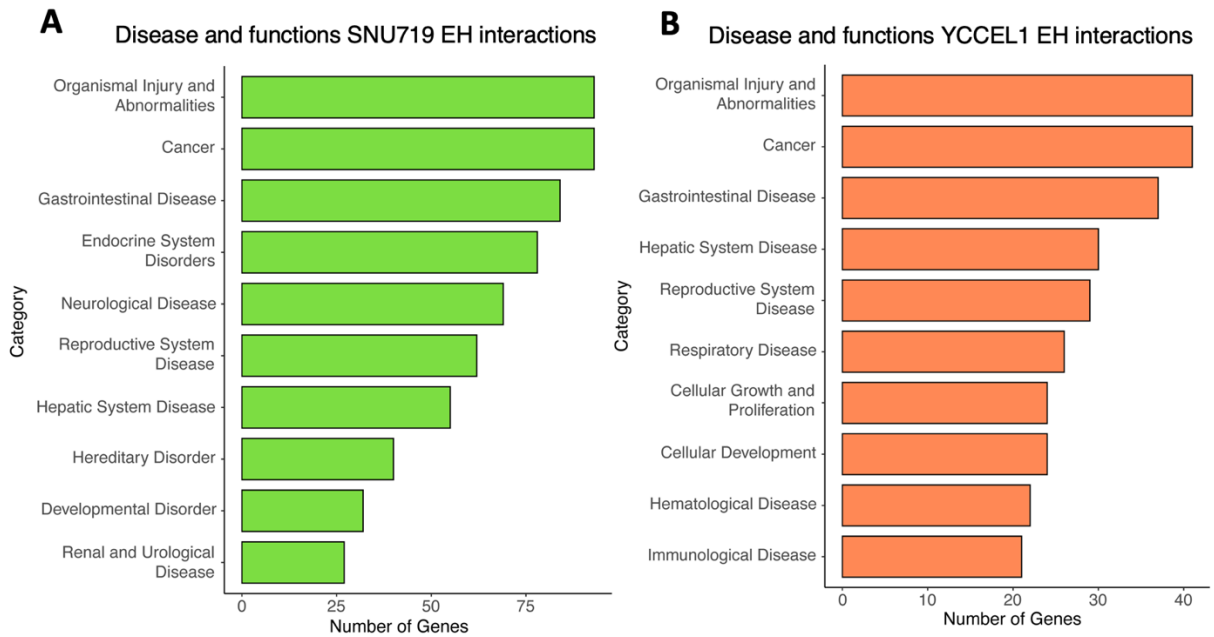


**Figure 33. A** Ingenuity Pathway Analysis (IPA) of genes found near EBV-Human interaction sites in SNU719 cell line. **B** IPA (as described in A) of genes found near EBV-Human interaction sites in YCCEL1 cell line.

Collectively, these findings strongly suggest that the presence of strong viral enhancers in proximity to specific genes leads to their overexpression (as depicted in Fig. 34). This, in turn, may play a critical role in the neoplastic transformation of the cells. The data provide valuable insights into the molecular mechanisms by which EBV enhancers can influence the host gene expression and potentially contribute to the development of gastric cancers in EBV-infected individuals.

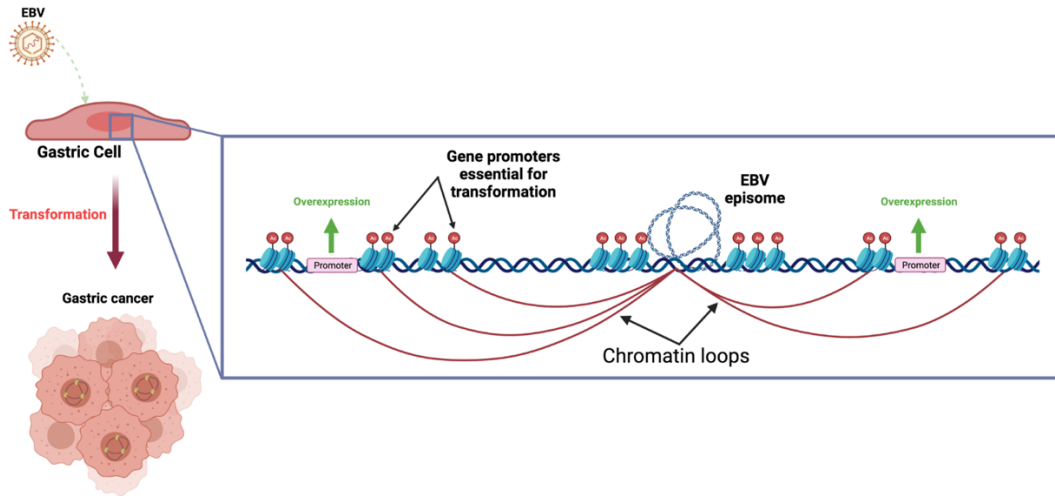


**Figure 34.** Model of the supposed mechanism of EBV-driven cell transformation. The figure was created with BioRender.com.

## 4. Discussion

In recent years, a growing body of research, including a recent study conducted by our group, has highlighted the significance of the three-dimensional structure of the EBV genome in governing viral gene expression (Morgan et al. 2022; Tempera, Klichinsky, and Lieberman 2011; Caruso, Maestri, and Tempera 2023). However, most of these earlier studies have primarily focused on characterizing the viral genome architecture within B cells, where EBV expresses either the highly restricted latency I program or the more permissive latency III program. Consequently, remains a considerable knowledge gap concerning the essential role, if any, played by the 3D EBV structure in epithelial cells, such as EBV+ gastric cancer cells, wherein the virus adopts a type II latency program. To address this gap, our present study aimed to explore the extent of this dependence in epithelial infected cells that exhibit a type II latency program. Through our studies, we aimed to shed light on the significance of the three-dimensional EBV genome structure in this specific cellular context.

Our findings reveal the crucial role of the 3D structure of the viral episome in EBV latency, with each EBV latency program characterized by a distinct three-dimensional conformation of the viral episome. Moreover, the 3D structure changes according to the type of infected cell and to the type of gastric cancer considered as showed by Principal Component Analysis of the HiC assay. The YCCEL1 cell line, in fact, presents a structure markedly different from B cells, but not entirely identical to that of SNU719, which, on the contrary, presents a structure more similar to that found in EBV+ B cells. An intriguing observation we report is the correlation between the network of long-distance chromatin interactions occurring throughout the viral genome and the expression levels of viral latent genes. This suggests an intimate link between the 3D viral chromatin structure and the transcriptional state of underlying viral loci engaged in chromatin loops. These observations align with recent studies by Zhang et al. (2023) and Barshad et al. (2023), which demonstrate how RNA Pol II activity and transcription levels can influence the formation of chromatin loops (S. Zhang et al. 2023; Barshad et al. 2023). According to these studies, RNA Pol II pausing can facilitate Cohesin loading and blocking, thereby

promoting the formation of enhancer-promoter loops. Notably, research from Dr. West's group (Palermo, Webb, and West 2011) has shown that RNA Pol II stalling occurs at the Cp promoter, and this stalling is essential for Cp activation and B cell immortalization. Considering these findings, it is tempting to speculate that differences in transcriptional activation and RNA Pol II activity across the EBV genome, coupled with Cohesin complex and CTCF binding at viral loci, may enable viral enhancer regions to actively scan neighboring chromatin regions for functional elements and generate different sets of chromatin loops. Such interplay between the 3D viral chromatin structure and transcriptional regulation could play a pivotal role in EBV's ability to maintain latency and influence its pathogenicity.

Given that chromatin loops connect functional genomic regions, our study further delved into the presence of functional elements across the EBV genome in epithelial cells, leading to the identification of novel potential viral enhancers. In both EBV+ gastric cancer cell lines, we observed an enrichment of histone modifications typical of enhancers, namely H3K4me1 and H3K27ac, at specific loci of the viral genome. An intriguing finding emerged from our analysis, as we not only identified enhancer signatures at well-known EBV functional regions like OriP, Cp, and Qp but also uncovered a chromatin enhancer signature at viral loci that are usually inactive during latency, such as Zp, OriLyt, and the LMP promoter adjacent to the TR regions. The use of HiChIP assay, which allowed us to assess chromatin loops mediated by H3K27ac, indicative of enhancer-promoter interactions, revealed that these putative novel viral enhancers are indeed engaged in chromatin loops that connect with viral promoters and are associated with CTCF occupancy. Specifically, we detected strong enhancer regions at the BILF2 gene promoter and the Qp promoter, both active in Type I and II latency programs. However, one surprising result was the observed differences in enhancer-promoter loops between the YCCEL1 and SNU719 cell lines, as evidenced by PCA analysis. The SNU719 cell line displayed multiple interactions, whereas the YCCEL1 cell line only exhibited three frequent interactions. These discrepancies might be attributed to differences in the origin of the cells (i.e., primary tumor versus metastatic lesion). Nevertheless, these findings indicate that 3D chromatin studies unveil novel and unexplored functional regions across

the viral genome in epithelial cells. Our results align with the recent work of Dr Zhao group, who conducted a similar HiChIP analysis in EBV+ B cells and identified novel potential enhancer-promoter loops involving similar regions (Ding et al. 2022). Collectively, these findings enhance our understanding of the dynamic interplay between chromatin architecture and viral gene regulation in different cellular contexts, providing valuable insights into EBV pathogenesis in epithelial cells. However, how different enhancer-promoter chromatin loops are established and maintained between different EBV latency type and EBV-infected cells of different cellular origin is still unknown and we plan to investigate it in the future.

Regarding the mechanisms controlling EBV chromatin, this study reaffirms the crucial role of PARP1 activity in the regulation of EBV chromatin architecture. Notably, our findings demonstrate that inhibiting PARP1 in both epithelial EBV+ cell lines resulted in the destabilization of CTCF binding across the viral genome, leading to significant alterations in the 3D chromatin structure of the EBV episome. These observations are consistent with our previous work on EBV+ B cells, where PARP1 inhibition was shown to epigenetically destabilize type III latency (Morgan et al. 2022; Lupey-Green et al. 2017; 2018). However, some divergences were observed between EBV+ B cells and EBV+ epithelial cells. In EBV+ gastric cancer cells, we noticed that Cohesin binding seemed to be randomly deregulated, suggesting a direct dependence between PARP1 activity and Cohesin binding. Unlike Type I and III latencies observed in B cells, in EBV+ GC cells, we observed an overall increase in short-range interactions in both cell lines, with a particularly prominent effect in the YCCEL1 cell line compared to SNU719 which could potentially be explained by their distinct origins (Oh et al. 2004; D. N. Kim et al. 2013). Similar to our observations in EBV+ B cells, the changes in 3D viral chromatin structure resulting from PARP1 inhibition in EBV+ epithelial cells also led to the repression of latent viral gene expression. Notably, these changes did not induce lytic reactivation, indicating that alterations in the 3D chromatin viral architecture are necessary but not sufficient to trigger EBV lytic replication (Tempera, Deng, et al. 2010; Mattiussi et al. 2007). Further research is necessary to unravel the intricate relationship between epigenetic

modifications and chromatin loop formation, and their role in regulating the lytic reactivation of EBV.

Furthermore, our aim was to gain a deeper understanding of the correlation between the presence of EBV and the transformation process leading to the tumorigenic fate of infected cells (K.-D. Kim et al. 2020; Okabe et al. 2020; Kumar et al. 2022). Employing the HiChIP assay, we not only identified EBV-host genomic interactions mediated by H3K27ac but also investigated the potential impact of strong active enhancers of EBV on neighboring oncogenes, possibly resulting in their overexpression and subsequent cell transformation. In our analysis, we discovered a prominent enhancer region near the BILF2 gene, along with the well-known OriP and LMP regions, as major sites of EBV-host interactions. Notably, genes near these interaction points were found to be markers of gastric tumors based on Ingenuity Pathway Analysis (IPA). Comparative assessment with a random set of control genes revealed significantly higher expression levels of these genes, in the SNU719 RNA-seq data, GES RNA-seq datasets and in biopsy samples from patients deposited in The Cancer Genome Atlas (TCGA)(The Cancer Genome Atlas Research Network 2014). These findings indicate a clear association between these tumors and EBV infection, even though similar overexpression of these genes is observed in EBV-negative gastric tumors, serving as a characteristic marker of this tumor type. It is plausible to hypothesize that the etiologic agent responsible for inducing their marked overexpression differs in these two cases.

This study reinforces the importance of the CTCF/Cohesin complex in governing the three-dimensional structure of the viral genome during EBV infection. This observation may have broader implications beyond EBV biology and could extend to other herpes viruses. Dr. Bloom and Dr. Neumann's research on HSV-1, along with Dr. Izumiya's work on KSHV, and findings from other groups, suggest that CTCF/Cohesin plays a role in regulating the 3D viral structure in various viruses, including HCMV, HPV, and HTLV-1 (Campbell et al. 2022; Elder et al. 2021; Ertel et al. 2012; Kang et al. 2011; Kang and Lieberman 2009; D.-J. Li et al. 2014; D. Li et al. 2020; Martinez et al. 2019; Martínez et al. 2014; Mehta et al. 2015; Paris et al. 2015; Pentland et al. 2018; Stedman et al. 2008;

Washington, Edenfield, et al. 2018; Washington, Musarrat, et al. 2018; Watson et al. 2018). Understanding if CTCF acts similarly across these viruses or if there are differences presents an intriguing area for further research particularly in the DNA viruses field.

However, it is important to acknowledge some limitations in this work. A major constraint of this study is the relatively small scale at which the CTCF/Cohesin/PARP1 crosstalk is observed, spanning only approximately 170 kb. This limited scope may not fully capture the complexities present in the Human genome at a megabase scale (Rao et al. 2014; K. Zhang et al. 2016; Rowley and Corces 2018). Additionally, the Hi-C assay, while providing valuable insights, is performed on a population of EBV+ cells, where each cell contains multiple episomes. This makes it challenging to discern the individual three-dimensional structures of each individual episome. Furthermore, our study is complicated by recent findings from our group (Preston-Alp et al. 2023), which reveal the presence of two populations of episomes in these EBV+ gastric cancer cell lines, each exhibiting distinct methylation patterns. This divergence could potentially account for the marked dissimilarities we observed in Cohesin binding and the extensive genome reorganization following treatment with a PARP1 inhibitor. Given these limitations, future investigations on larger genomic scales and single-cell level analyses may offer a more comprehensive understanding of the complex interactions involving CTCF, Cohesin, and PARP1 in EBV-infected cells. Moreover, addressing the impact of distinct episome populations and their methylation patterns could lead to a deeper appreciation of the observed effects in the context of EBV-associated gastric cancer.

## **5. Conclusions**

In summary, our study underscores the significance of PARP1 activity in shaping EBV chromatin architecture, providing valuable insights into the mechanisms underlying viral latency regulation. Moreover, the differences observed between EBV+ B cells and EBV+ epithelial cells emphasize the complexity of chromatin dynamics and its context-specific nature in different cell types, shedding light on the intricate interplay between PARP1, CTCF, and Cohesin in the control of EBV gene expression. In addition, our research reveals the intricate interplay between EBV infection, chromatin interactions, and oncogene expression in the context of gastric tumors. The identification of potential mechanisms underlying the transformation process enhances our understanding of EBV-associated tumorigenesis and opens new avenues for further investigation into the role of viral enhancers in promoting oncogene expression and cellular transformation.

## **6. Materials and Methods**

### **Cell culture and treatment**

Cell lines were maintained in a humidified incubator containing 5% CO<sub>2</sub> at 37 °C. YCCEL1, SNU719 and Mutu1 cell lines were cultured in RPMI 1640 supplemented with Fetal Bovine Serum at a concentration of 10% and supplemented with 1% penicillin-streptomycin. LCL cell lines were cultured in RPMI 1640 supplemented with Fetal Bovine Serum at a concentration of 15% and supplemented with 1% penicillin-streptomycin.

Treatment with PARP inhibitor Olaparib (Selleck Chemicals, Catalog No. S1060) was given 72 h before collection at a concentration of 5 µM.

### **Dot Blot**

Dot Blot was carried out as per Abcam protocol. Briefly, three biological replicates of 2x10<sup>6</sup> YCCEL1/SNU719 cells per treatment group (with or without 5 µM Olaparib for 72 h) were extracted using radioimmunoprecipitation assay (RIPA) lysis buffer (50 mM Tris-HCl, pH 7.4, 150 mM NaCl, 0.25% deoxycholic acid, 1% NP-40, 1 mM EDTA; Millipore, cat. No. 20-188) supplemented with 1X protease inhibitor cocktail (Sigma-Aldrich, cat. No. P8340-5ML) and 1X PARG inhibitor (PDD00017273, Selleck Chemicals, catalog No. S8862). Protein concentration was measured using a bicinchoninic acid (BCA) protein assay (Pierce, cat. No. 23227) and 10 µg of protein were diluted in 50 µL of water and loaded onto the activated nitrocellulose membrane (Bio-Rad cat. No. 1620113).

Red Ponceau staining (Ponceau S Staining Solution, Cell Signaling, catalog No. 59803) was used as a loading control.

Membrane was blocked in 5% milk TBS-T and then incubated with anti-PAR antibody (R&D Systems, catalog No. 4335-MC-100) as per manufacturer recommendation.

Membrane was washed 5 mins three times, incubated for 1 h with rabbit anti-mouse IgG-HRP (Jackson ImmunoResearch), at a dilution of 1:10000 and detected by enhanced chemiluminescence (SuperSignal West Dura Extended Duration Substrate, catalog No. 34075).

### **Subcellular fractionation and Western Blot**

Three biological replicates of  $5 \times 10^6$  YCCEL1/SNU719 cells per treatment group (with or without  $5 \mu\text{M}$  Olaparib for 72 h) were prepared using the Subcellular Protein Fractionation Kit for Cultured Cells (Thermo Scientific, catalog No. 78840) as per manufacturer's protocol.

Protein concentration was measured using a bicinchoninic acid (BCA) protein assay (Pierce). Lysates were boiled with 2X Laemmli sample buffer (Bio-Rad, cat. No 1610737) containing 2.5%  $\beta$ -mercaptoethanol (Sigma-Aldrich, cat. No. M6250-100ML).

Proteins were resolved by gel electrophoresis on a 4-20% polyacrylamide gradient Mini-Protean TGX pre-cast gel (Bio-Rad, cat. No. 4561096) and transferred to an Immobilon-P membrane (Millipore, cat. No. IPVH00010) using a Power Blotter XL System (Invitrogen).

Membranes were blocked in 5% milk PBS-T for 1 h at room temperature and incubated overnight at  $4^\circ\text{C}$  with primary antibodies against SMC3 (Bethyl Laboratories A300-060A), SMC1 (Bethyl Laboratories A300-055A), Rad21 (Bethyl Laboratories A300-080A), CTCF (Active Motif 61311), PARP1 N-terminal (Active Motif 39559), and Histone H3 (Abcam ab1791) as per manufacturer recommendation. Membranes were washed 5 mins three times, incubated for 1 h with the appropriate secondary antibody, either goat anti-rabbit IgG-HRP (Jackson ImmunoResearch) or rabbit anti-mouse IgG-HRP (Jackson ImmunoResearch), at a dilution of 1:10000. Membranes were then washed and detected by enhanced chemiluminescence (SuperSignal West Dura Extended Duration Substrate).

### **Poly (ADP-Ribose) ELISA assay**

The ELISA assay to assess the levels of intracellular Poly (ADP-Ribose) (PAR) was carried out using  $7 \times 10^6$  cells per sample using the Poly (ADP-Ribose) ELISA kit (Cell Biolabs, cat. No. XDN-5114) as per manufacturer protocol.

### **RNA extraction and RNA-seq**

Total RNA from SNU719 cell line was isolated from  $2 \times 10^6$  cells using a Direct-zol RNA Kit (Zymo Research, cat. No. R2050) according to the manufacturer's protocol. RNA samples were either used for downstream RT-qPCR or submitted to the Wistar Institute

genomics core facility for RNA quality control and sequencing library preparation using the SENSE mRNA-Seq Library Prep Kit V2 (Lexogen) to generate Illumina-compatible sequencing libraries according to the manufacturer's instructions. Paired-end reads of 75 bp were obtained using a Illumina HiSeq 2500 sequencer. RNA-seq data was aligned using bowtie2(Langmead and Salzberg 2012) against hg19 version of the Human genome and all unaligned reads were then aligned against NC\_007605.1 version of EBV genome and RSEM v1.2.12 software (B. Li and Dewey 2011) was used to estimate raw read counts and RPKM for Human and EBV genes.

Datasets are available in Gene Expression Omnibus see Data Availability section for accession number.

### RT-qPCR

For quantitative reverse transcription-PCR (RT-qPCR), SuperScript IV reverse transcriptase (Invitrogen, cat. no. 18090200) was used to generate randomly primed cDNA from 1 µg of total RNA. 50 ng of cDNA sample was analyzed in triplicate by quantitative PCR using the ABI StepOnePlus system. Data were analyzed by the  $\Delta\Delta C_T$  method relative to 18S-ribosomal subunit control. Primer sequences are listed below:

<b>Name</b>	<b>Sequence</b>
EBNA1 Fw	GGTCGTGGACGTGGAGAAAA
EBNA1 Rev	GGTGGAGACCCGGATGATG
LMP2B Rev	GGCGGTCACAACGGTACTAACT
LMP2B Fw	CGGGAGGCCGTGCTTTAG
BMRF1 Fw	TTGGGCAGGTGCTGTTGAT
BMRF1 Rev	TGCCCACTTCTGCAACGA
SMC3 Fw	CGAGCAAGATGGAATTGGGGA
SMC3 Rev	GCTCATGGGTGACTCTCAACA
RAD21 Fw	GGATAAGAAGCTAACCAAAGCCC
RAD21 Rev	CTCCCAGTAAGAGATGTCCTGAT
STAG1 Fw	TGGCAGCGAGCTTGAAGAAA
STAG1 Rev	CCACCTCAAATAATGTGACAGGC
SMC1 Fw	AACCTGCGGGTAAAGACCCT
SMC1 Rev	GGCAAAGGTACGGTCCTCAG
CTCF Fw	AAGAAAGATGCGCTCTAAGAAAGA

## Chromatin immunoprecipitation assays

### Chromatin immunoprecipitation sequencing (ChIP-seq)

Chromatin immunoprecipitation with next-generation sequencing (ChIP-seq) was performed as previously described (Morgan et al. 2022). Briefly,  $25 \times 10^6$  cells per immunoprecipitation were collected and fixed with 1% formaldehyde for 15 min and then quenched with 0.25 M glycine for 5 min on ice. After 3 washes with 1X PBS, pellets were resuspended in 10 mL each of a series of two lysis buffers and resuspended in 1 mL of the third lysis buffer before fragmentation in Covaris ME220 Ultrasonicator (peak power 75, duty factor 25, cycles/burst 1000, average power 18.8, time 720 sec) to generate chromatin fragments roughly 200–500 bp in size. Chromatin was centrifuged to clear debris and a 1:20 of this cleared chromatin was kept as standard input for comparison against immunoprecipitations. Chromatin was incubated rotating at 4° 1h with 25 µg H3K4me1 (Active Motif 39299) and 25 µg H3K27ac (Active Motif 39133), then chromatin–antibody complexes were precipitated using 50 µL of Dynabeads Protein A (ThermoFisher, product No. 10001D) incubated rotating at 4° overnight. DNA was purified using Promega Wizard SV Gel and PCR Clean-up Kit (product No. A9285). Libraries for sequencing were made using NEBNext Ultra II DNA Library Prep Kit (New England Biolabs, product No. E7103) and sequenced on the Illumina HiSeq 2500.

### ChIP-seq analysis

Reads were mapped against the human gammaherpesvirus 4 (HHV4) NC\_007605.1 genome assembly and hg19 Human genome assembly using Burrows-Wheeler Aligner (BWA) (H. Li and Durbin 2010). We used MACS2 (Feng et al. 2012; Y. Zhang et al. 2008) software package to call peaks using input samples as control. deepTools (Ramírez et al. 2016) was used for data visualization.

For transcription factor binding motif analysis, Analysis of Motif Enrichment (AME) from the MEME-ChIP suite (Bailey et al. 2015) and *findMotifsGenome.pl* pipeline from HOMER package (Heinz et al. 2010) were used using default options.

ChIP-seq data were deposited for public access at Gene Expression Omnibus see Data Availability section for accession number.

### **Chromatin immunoprecipitation (ChIP)**

Chromatin immunoprecipitation was performed as previously described (Morgan et al. 2022) with minor changes. Briefly, after 72 h incubation with or without Olaparib,  $1 \times 10^6$  cells per immunoprecipitation reaction were collected and fixed with 1% formaldehyde for 15 min and then quenched with 0.125 M glycine for 5 min on ice. After centrifugation, the pellet was washed three times in 1X PBS and after the final wash resuspended in 120  $\mu$ L SDS Lysis Buffer (1% SDS, 10mM EDTA, 50mM Tris pH 8.0) and sonicated using Covaris ME220 Ultrasonicator (peak power 75, duty factor 25, cycles/burst 1000, average power 18.8, time 600 sec) to generate chromatin fragments roughly 100–200 bp in size. The success of the sonication was checked running 15  $\mu$ L of sonicated chromatin on a 1% agarose gel after de-crosslink and purification using the Zymo DNA Clean and Concentrator-5 kit (Zymo Research). Chromatins were then diluted in IP Dilution Buffer (0.001% SDS, 1.1% Triton X-100, 1.2mM EDTA, 16.7 mM Tris pH 8.0, 150mM NaCl). A sample of “input chromatin” was collected at this point as a standard for comparison against immunoprecipitations (5% of total material). Chromatin was then incubated overnight rotating at 4° with 4  $\mu$ g of antibody against CTCF, 5  $\mu$ g of antibody against SMC1 and 5  $\mu$ g of IgG antibody. The next day 45  $\mu$ L of Dynabeads Protein A were added to each reaction and rotated for 2 hours. Beads were washed five times by adding sequentially Low Salt Wash Buffer (0.1% SDS, 1% Triton X-100, 2mM EDTA, 20mM Tris pH 8.0, 150mM NaCl), High Salt Wash Buffer (0.1% SDS, 1% Triton X-100, 2mM EDTA, 20mM Tris pH 8.0, 500mM NaCl), LiCl Wash Buffer (250mM LiCl, 1% NP-40, 1% Na-deoxycholate, 1mM EDTA, 10mM Tris pH 8.0), twice TE Buffer (1mM EDTA, 10mM Tris pH 8.0). Chromatin-protein complexes were eluted from the beads by adding 150  $\mu$ L of TE/1% SDS and shook on a Thermoblock for 15 minutes at 65°C. DNA was de-crosslinked overnight and purified using the Promega Wizard SV Gel and PCR Clean-up Kit.

Real-time PCR was performed with a master mix containing 1X Maxima SYBR Green (Thermoscientific, REF No. K0223), 0.25  $\mu$ M primers and 1:50 of ChIP or input DNA per

well. Quantitative PCRs were carried out in triplicate using the ABI StepOnePlus PCR system. Data were analyzed by the  $\Delta\Delta CT$  method (where CT is threshold cycle) relative to DNA input. Primer sequences are listed below:

<b>Name</b>	<b>Sequence</b>
CTCF Eber Fw	GGGTTCCCAGAGAGGGTAAA
CTCF Eber Rev	GGGTTTGCTATAGTTGGTGTGTAG
CTCF Cp Fw	CACTCGCCCACTAACCTTAAC
CTCF Cp Rev	GGCCTGTAGTTTCGCATCTT
CTCF Qp Fw	CACCTCCCTGATAATGTCTTCAA
CTCF Qp Rev	ACCAGACAACATTACTGTGGAA
CTCF BZLF1 Fw	CTGTCATGGACTCTAGTGTTGTG
CTCF BZLF1 Rev	AGAAGGAGGAAGCAGCCATA
CTCF RMPS1 Fw	ATGCAAGTGCATCTTTCTAACC
CTCF RMPS1 Rev	CACAGCACTCCCACTAGTTC
CTCF LMP Fw	ATTGCAACACGACGGGAATG
CTCF LMP Rev	CTCTGCCCGCTTCTTCGTAT

## **Chromatin Conformation Capture Assays**

### **HiC assay**

Hi-C assay was performed as previously described (Morgan et al. 2022). Briefly,  $5 \times 10^6$  cells per condition were collected for *in-situ* Hi-C. Libraries of total ligation products were produced using Ultralow Library Systems V2 (Tecan Genomics, part no. 0344NB-32) as per manufacturer's protocol.

For the additional enrichment of EBV DNA, purified libraries were then enriched for only EBV genome ligation products using myBaits enrichment kit as per manufacturer's protocol. Libraries were sequenced using the Illumina HiSeq 2500 sequencing platform with paired-end 75bp read length. HiC data was preprocessed using HiC-Pro v2.10.0 pipeline (Servant et al. 2015) with default settings using NC\_007605.1 version of the EBV genome at 1kb resolution. DESeq2 (Love, Huber, and Anders 2014) was used to estimate significance of differential contact based on raw count matrix files. Significantly changed associations (FDR<5%) were plotted as circos graph using the circlize package (version 0.4.12) of R (version 4.0.5) (Gu et al. 2014).

To identify cell-type specific loops we summed all the interactions that passed the FDR threshold based on cell type and further filtered them by CTCF binding. Then a differential analysis was performed using DESeq2 R package as described above.

The detailed protocol with all minor alterations will be happily supplied by corresponding author per request. Datasets are available in GEO see Data Availability section for the accession number.

### **HiChIP assay**

HiChIP assay was performed as per protocol (Mumbach et al. 2016) with minor changes. Briefly,  $25 \times 10^6$  cells were fixed with 1% formaldehyde for 10 min and then quenched with 0.125 M glycine for 5 min at RT. Ligation products were immunoprecipitated with 25  $\mu$ g H3K27ac (Active Motif 39133). 5  $\mu$ L of Streptavidin C-1 beads were used for biotin pull-down. After the last wash with Tween Wash Buffer bead-bound DNA was used to prepare libraries with Ultralow Library Systems V2 (Tecan Genomics, part no. 0344NB-32) as per manufacturer's protocol.

Libraries were then deep sequenced using the Illumina HiSeq 2500 sequencing platform. Data was preprocessed using HiC-Pro v2.10.0 pipeline (Servant et al. 2015) with default settings using NC\_007605.1 version of the EBV genome at 5kb resolution and *hichipper* software (C. Lareau and Aryee 2017) was used to perform restriction site bias modeling and interaction identification.

Only statistically significant interactions (FDR<5%) were kept for downstream analysis.

Differential interactions between cell lines were identified using the *diffloop* Bioconductor R package (C. A. Lareau and Aryee 2018). Significantly changed associations (FDR<1%) were used for visualization in UCSC Genome Browser.

To identify EBV-Human interactions, the output of *hichipper* software was filtered for those interactions having more than 2 reads, than they were plotted using the *circlize* R package (Gu et al. 2014). H3K27ac peaks in proximity to EBV-Human interactions were annotated using the HOMER software (Heinz et al. 2010) and filtered for just those genes which Transcription Start Sites (TSS) were within 1 kb from the peak.

Transcription factor binding motif analysis was carried out using Analysis of Motif Enrichment (AME) from the MEME-ChIP suite (Bailey et al. 2015) with default options.

### **Droplet Digital PCR (ddPCR)**

Multiplex DNA droplet PCR (ddPCR) was performed as previously described (Lin et al. 2016). DNA was isolated from  $1 \times 10^6$  cells using the GeneJET Genomic DNA Purification Kit (Thermo Scientific) according to the manufacturer's protocol. 500 ng of DNA was digested with BamHI enzyme (10 U/ $\mu$ l, New England Biolabs) in a total volume of 10  $\mu$ l for 1 hour at 37°C. Digestion was diluted 1:20 in nuclease-free water. 10  $\mu$ l of diluted DNA digest was mixed with 12.5  $\mu$ l of 2x digital PCR supermix for probes (No dUTP) (Bio-Rad), 1.25  $\mu$ l 20x FAM primers, 1.25  $\mu$ l VIC primers for each reaction. The FAM primers sequence for EBV Lmp1 was Fw(5'-3') AAGGTCAAAGAACAAGGCCAAG, Rv (5'-3') GCATCGGAGTCGGTGG, and FAM- AGCGTGTCCCCGTGGAGG.

Host control primer sequence for Ribonuclease P protein subunit 30 (Rpp30) was Fw (5'-3') GATTTGGACCTGCGAGCG, Rv (5'-3') GCGGCTGTCTCCACAAGT, and probe VIC-CTGACCTGAAGGCTCT. 20x primers contain 18  $\mu$ M PCR primers and 5  $\mu$ M probes for a final PCR reaction concentration of 900 nM PCR primers and 250 nM probe. Each sample was run in duplicate. The ddPCR plate was sealed with a foil heat seal using the PX1 PCR Plate Sealer (Bio-Rad) at 180°C for 5 sec. The plate was vortexed and spun down at 1000rpm for 1 min. Droplets were generated using the QX200 Droplet Digital PCR System (Bio-Rad) and transfer of emulsified samples to a PCR plate was performed according to manufacturer's instructions. PCR plate containing emulsified droplets was sealed with a foil heat seal. PCR reactions were performed on the C1000 Touch Thermal Cycler (Bio-Rad). The cycling protocol included an enzyme activation step at 95°C for 10 min and cycled 40 times between a denaturing step at 94°C for 30 sec and an annealing and extension step at 60°C for 1 min, finally one enzyme deactivation step was performed at 98°C for 10. The ramp rate between these steps set at 2°C/sec. Droplets were then counted using QX200 Droplet Reader (Bio-Rad). The absolute quantity of DNA per sample was determined using the QuantaSoft software.

## **Statistical analysis**

All experiments presented were conducted at least in triplicate to ensure reproducibility of results. The Prism statistical software package (GraphPad) was used to identify statistically significant differences between experimental conditions and control samples, using *Student's t test* as indicated in the figure legends.

## **Data Availability**

The data that support this study are available from the corresponding author upon reasonable request. The data for the HiC assay, ChIP-seq assay for H3K27ac, H3K4me1, RNA-seq for SNU719 and the H3K27ac HiChIP have been deposited in the Gene Expression Omnibus database under the following accession code GSE239995. ChIP-seq experiments for CTCF in Mutu1, LCL and Gastric Cancer cells were obtained by publicly available sequencing datasets [GSE115829](#), [GSE160973](#), [GSE234603](#), generated in our previous works. RNA-seq datasets on GES cells before and after EBV infection are available on Gene Expression Omnibus under the accession code [GSE147152](#).

## 7. References

- Abbot, S D, M Rowe, K Cadwallader, A Ricksten, J Gordon, F Wang, L Rymo, and A B Rickinson. 1990. "Epstein-Barr Virus Nuclear Antigen 2 Induces Expression of the Virus-Encoded Latent Membrane Protein." *Journal of Virology* 64 (5): 2126–34. <https://doi.org/10.1128/jvi.64.5.2126-2134.1990>.
- Ambinder, Richard F., Keith D. Robertson, and Qian Tao. 1999. "DNA Methylation and the Epstein–Barr Virus." *Seminars in Cancer Biology* 9 (5): 369–75. <https://doi.org/10.1006/scbi.1999.0137>.
- Arvey, Aaron, Italo Tempera, and Paul Lieberman. 2013. "Interpreting the Epstein-Barr Virus (EBV) Epigenome Using High-Throughput Data." *Viruses* 5 (4): 1042–54. <https://doi.org/10.3390/v5041042>.
- Arvey, Aaron, Italo Tempera, Kevin Tsai, Horng-Shen Chen, Nadezhda Tikhmyanova, Michael Klichinsky, Christina Leslie, and Paul M. Lieberman. 2012. "An Atlas of the Epstein-Barr Virus Transcriptome and Epigenome Reveals Host-Virus Regulatory Interactions." *Cell Host & Microbe* 12 (2): 233–45. <https://doi.org/10.1016/j.chom.2012.06.008>.
- Bailey, Timothy L., James Johnson, Charles E. Grant, and William S. Noble. 2015. "The MEME Suite." *Nucleic Acids Research* 43 (W1): W39–49. <https://doi.org/10.1093/nar/gkv416>.
- Barshad, Gilad, James J. Lewis, Alexandra G. Chivu, Abderhman Abubashem, Nils Krietenstein, Edward J. Rice, Yitian Ma, et al. 2023. "RNA Polymerase II Dynamics Shape Enhancer–Promoter Interactions." *Nature Genetics*, July. <https://doi.org/10.1038/s41588-023-01442-7>.
- Bell, Adam C, Adam G West, and Gary Felsenfeld. 1999. "The Protein CTCF Is Required for the Enhancer Blocking Activity of Vertebrate Insulators." *Cell* 98 (3): 387–96. [https://doi.org/10.1016/S0092-8674\(00\)81967-4](https://doi.org/10.1016/S0092-8674(00)81967-4).
- Bergbauer, Martin, Markus Kalla, Anne Schmeinck, Christine Göbel, Ulrich Rothbauer, Sebastian Eck, Anna Benet-Pagès, Tim M. Strom, and Wolfgang Hammerschmidt. 2010. "CpG-Methylation Regulates a Class of Epstein-Barr Virus Promoters."

- Edited by Samuel H. Speck. *PLoS Pathogens* 6 (9): e1001114. <https://doi.org/10.1371/journal.ppat.1001114>.
- Bochum, Sylvia, Stephanie Berger, and Uwe M. Martens. 2018. "Olaparib." In *Small Molecules in Oncology*, edited by Uwe M. Martens, 211:217–33. Recent Results in Cancer Research. Cham: Springer International Publishing. [https://doi.org/10.1007/978-3-319-91442-8\\_15](https://doi.org/10.1007/978-3-319-91442-8_15).
- Bray, Freddie, Jacques Ferlay, Isabelle Soerjomataram, Rebecca L. Siegel, Lindsey A. Torre, and Ahmedin Jemal. 2018. "Global Cancer Statistics 2018: GLOBOCAN Estimates of Incidence and Mortality Worldwide for 36 Cancers in 185 Countries." *CA: A Cancer Journal for Clinicians* 68 (6): 394–424. <https://doi.org/10.3322/caac.21492>.
- Brink, A A, D F Dukers, A J Van Den Brule, J J Oudejans, J M Middeldorp, C J Meijer, and M Jiwa. 1997. "Presence of Epstein-Barr Virus Latency Type III at the Single Cell Level in Post-Transplantation Lymphoproliferative Disorders and AIDS Related Lymphomas." *Journal of Clinical Pathology* 50 (11): 911–18. <https://doi.org/10.1136/jcp.50.11.911>.
- Buschle, Alexander, and Wolfgang Hammerschmidt. 2020. "Epigenetic Lifestyle of Epstein-Barr Virus." *Seminars in Immunopathology* 42 (2): 131–42. <https://doi.org/10.1007/s00281-020-00792-2>.
- Camargo, M C, G Murphy, C Koriyama, R M Pfeiffer, W H Kim, R Herrera-Goepfert, A H Corvalan, et al. 2011. "Determinants of Epstein-Barr Virus-Positive Gastric Cancer: An International Pooled Analysis." *British Journal of Cancer* 105 (1): 38–43. <https://doi.org/10.1038/bjc.2011.215>.
- Campbell, Mel, Chanikarn Chantarasrivong, Yuichi Yanagihashi, Tomoki Inagaki, Ryan R. Davis, Kazushi Nakano, Ashish Kumar, Clifford G. Tepper, and Yoshihiro Izumiya. 2022. "KSHV Topologically Associating Domains in Latent and Reactivated Viral Chromatin." Edited by Jae U. Jung. *Journal of Virology* 96 (14): e00565-22. <https://doi.org/10.1128/jvi.00565-22>.
- Caruso, Lisa Beatrice, Davide Maestri, and Italo Tempera. 2023. "Three-Dimensional Chromatin Structure of the EBV Genome: A Crucial Factor in Viral Infection." *Viruses* 15 (5): 1088. <https://doi.org/10.3390/v15051088>.

- Chau, Charles M., Xiao-Yong Zhang, Steven B. McMahon, and Paul M. Lieberman. 2006. "Regulation of Epstein-Barr Virus Latency Type by the Chromatin Boundary Factor CTCF." *Journal of Virology* 80 (12): 5723–32. <https://doi.org/10.1128/JVI.00025-06>.
- Chen, Horng-Shen, Kayla A. Martin, Fang Lu, Lena N. Lupey, Joshua M. Mueller, Paul M. Lieberman, and Italo Tempera. 2014. "Epigenetic Deregulation of the LMP1/LMP2 Locus of Epstein-Barr Virus by Mutation of a Single CTCF-Cohesin Binding Site." *Journal of Virology* 88 (3): 1703–13. <https://doi.org/10.1128/JVI.02209-13>.
- Chiang, Alan K.S., Qian Tao, Gopesh Srivastava, and Faith C.S. Ho. 1996. "Nasal NK- and T-Cell Lymphomas Share the Same Type of Epstein-Barr Virus Latency as Nasopharyngeal Carcinoma and Hodgkin's Disease." *International Journal of Cancer* 68 (3): 285–90. [https://doi.org/10.1002/\(SICI\)1097-0215\(19961104\)68:3<285::AID-IJC3>3.0.CO;2-Y](https://doi.org/10.1002/(SICI)1097-0215(19961104)68:3<285::AID-IJC3>3.0.CO;2-Y).
- Cristescu, Razvan, Jeeyun Lee, Michael Nebozhyn, Kyoung-Mee Kim, Jason C Ting, Swee Seong Wong, Jiangang Liu, et al. 2015. "Molecular Analysis of Gastric Cancer Identifies Subtypes Associated with Distinct Clinical Outcomes." *Nature Medicine* 21 (5): 449–56. <https://doi.org/10.1038/nm.3850>.
- Day, Latasha, Charles M. Chau, Michael Nebozhyn, Andrew J. Rennekamp, Michael Showe, and Paul M. Lieberman. 2007. "Chromatin Profiling of Epstein-Barr Virus Latency Control Region." *Journal of Virology* 81 (12): 6389–6401. <https://doi.org/10.1128/JVI.02172-06>.
- Degner, Stephanie C., Jiyoti Verma-Gaur, Timothy P. Wong, Claudia Bossen, G. Michael Iverson, Ali Torkamani, Christian Vettermann, et al. 2011. "CCCTC-Binding Factor (CTCF) and Cohesin Influence the Genomic Architecture of the *Igh* Locus and Antisense Transcription in pro-B Cells." *Proceedings of the National Academy of Sciences* 108 (23): 9566–71. <https://doi.org/10.1073/pnas.1019391108>.
- Degner, Stephanie C., Timothy P. Wong, Gytis Jankevicius, and Ann J. Feeney. 2009. "Cutting Edge: Developmental Stage-Specific Recruitment of Cohesin to CTCF Sites throughout Immunoglobulin Loci during B Lymphocyte Development." *The Journal of Immunology* 182 (1): 44–48. <https://doi.org/10.4049/jimmunol.182.1.44>.

- Ding, Weiyue, Chong Wang, Yohei Narita, Hongbo Wang, Merrin Man Long Leong, Alvin Huang, Yifei Liao, et al. 2022. "The Epstein-Barr Virus Enhancer Interaction Landscapes in Virus-Associated Cancer Cell Lines." Edited by Lori Frappier. *Journal of Virology* 96 (18): e00739-22. <https://doi.org/10.1128/jvi.00739-22>.
- Dunmire, Samantha K., Priya S. Verghese, and Henry H. Balfour. 2018. "Primary Epstein-Barr Virus Infection." *Journal of Clinical Virology* 102 (May): 84–92. <https://doi.org/10.1016/j.jcv.2018.03.001>.
- Elder, Elizabeth G., Benjamin A. Krishna, Emma Poole, Marianne Perera, and John Sinclair. 2021. "Regulation of Host and Viral Promoters during Human Cytomegalovirus Latency via US28 and CTCF." *Journal of General Virology* 102 (5). <https://doi.org/10.1099/jgv.0.001609>.
- Epstein, M.A, B.G Achong, and Y.M Barr. 1964. "VIRUS PARTICLES IN CULTURED LYMPHOBLASTS FROM BURKITT'S LYMPHOMA." *The Lancet* 283 (7335): 702–3. [https://doi.org/10.1016/S0140-6736\(64\)91524-7](https://doi.org/10.1016/S0140-6736(64)91524-7).
- Ertel, Monica K., Amy L. Cammarata, Rebecca J. Hron, and Donna M. Neumann. 2012. "CTCF Occupation of the Herpes Simplex Virus 1 Genome Is Disrupted at Early Times Postreactivation in a Transcription-Dependent Manner." *Journal of Virology* 86 (23): 12741–59. <https://doi.org/10.1128/JVI.01655-12>.
- Falk, Kerstin I., Laszlo Szekely, Anna Aleman, and Ingemar Ernberg. 1998. "Specific Methylation Patterns in Two Control Regions of Epstein-Barr Virus Latency: The LMP-1-Coding Upstream Regulatory Region and an Origin of DNA Replication (oriP)." *Journal of Virology* 72 (4): 2969–74. <https://doi.org/10.1128/JVI.72.4.2969-2974.1998>.
- Farrar, Dawn, Sushma Rai, Igor Chernukhin, Maja Jagodic, Yoko Ito, Samer Yammine, Rolf Ohlsson, Adele Murrell, and Elena Klenova. 2010. "Mutational Analysis of the Poly(ADP-Ribosyl)ation Sites of the Transcription Factor CTCF Provides an Insight into the Mechanism of Its Regulation by Poly(ADP-Ribosyl)ation." *Molecular and Cellular Biology* 30 (5): 1199–1216. <https://doi.org/10.1128/MCB.00827-09>.

- Farrell, Paul J. 2019. "Epstein–Barr Virus and Cancer." *Annual Review of Pathology: Mechanisms of Disease* 14 (1): 29–53. <https://doi.org/10.1146/annurev-pathmechdis-012418-013023>.
- Feng, Jianxing, Tao Liu, Bo Qin, Yong Zhang, and Xiaole Shirley Liu. 2012. "Identifying ChIP-Seq Enrichment Using MACS." *Nature Protocols* 7 (9): 1728–40. <https://doi.org/10.1038/nprot.2012.101>.
- Gedder, Helene, Axel Zur Hausen, Helmut E. Gabbert, and Mario Sarbia. 2010. "EBV-Infection in Cardiac and Non-Cardiac Gastric Adenocarcinomas Is Associated with Promoter Methylation of *P16*, *P14* and *APC*, but Not *hMLH1*." *Analytical Cellular Pathology* 33 (3–4): 143–49. <https://doi.org/10.1155/2010/453764>.
- Gu, Zuguang, Lei Gu, Roland Eils, Matthias Schlesner, and Benedikt Brors. 2014. "Circlize Implements and Enhances Circular Visualization in R." *Bioinformatics* 30 (19): 2811–12. <https://doi.org/10.1093/bioinformatics/btu393>.
- Guo, Rui, Chang Jiang, Yuchen Zhang, Apurva Govande, Stephen J. Trudeau, Fang Chen, Christopher J. Fry, et al. 2020. "MYC Controls the Epstein-Barr Virus Lytic Switch." *Molecular Cell* 78 (4): 653–669.e8. <https://doi.org/10.1016/j.molcel.2020.03.025>.
- Heinz, Sven, Christopher Benner, Nathanael Spann, Eric Bertolino, Yin C. Lin, Peter Laslo, Jason X. Cheng, Cornelis Murre, Harinder Singh, and Christopher K. Glass. 2010. "Simple Combinations of Lineage-Determining Transcription Factors Prime Cis-Regulatory Elements Required for Macrophage and B Cell Identities." *Molecular Cell* 38 (4): 576–89. <https://doi.org/10.1016/j.molcel.2010.05.004>.
- Hodin, Theresa L., Tanbir Najrana, and John L. Yates. 2013. "Efficient Replication of Epstein-Barr Virus-Derived Plasmids Requires Tethering by EBNA1 to Host Chromosomes." *Journal of Virology* 87 (23): 13020–28. <https://doi.org/10.1128/JVI.01606-13>.
- Holdorf, Meghan M., Samantha B. Cooper, Keith R. Yamamoto, and Jj L. Miranda. 2011. "Occupancy of Chromatin Organizers in the Epstein–Barr Virus Genome." *Virology* 415 (1): 1–5. <https://doi.org/10.1016/j.virol.2011.04.004>.
- Hsu, Joe L, and Sally L Glaser. 2000. "Epstein–Barr Virus-Associated Malignancies: Epidemiologic Patterns and Etiologic Implications." *Critical Reviews in*

*Oncology/Hematology* 34 (1): 27–53. [https://doi.org/10.1016/S1040-8428\(00\)00046-9](https://doi.org/10.1016/S1040-8428(00)00046-9).

- Hughes, David J., Elessa M. Marendy, Carol A. Dickerson, Kristen D. Yetming, Clare E. Sample, and Jeffery T. Sample. 2012. “Contributions of CTCF and DNA Methyltransferases DNMT1 and DNMT3B to Epstein-Barr Virus Restricted Latency.” *Journal of Virology* 86 (2): 1034–45. <https://doi.org/10.1128/JVI.05923-11>.
- Jones, C H, S D Hayward, and D R Rawlins. 1989. “Interaction of the Lymphocyte-Derived Epstein-Barr Virus Nuclear Antigen EBNA-1 with Its DNA-Binding Sites.” *Journal of Virology* 63 (1): 101–10. <https://doi.org/10.1128/jvi.63.1.101-110.1989>.
- Kalla, Markus, Anne Schmeinck, Martin Bergbauer, Dagmar Pich, and Wolfgang Hammerschmidt. 2010. “AP-1 Homolog BZLF1 of Epstein–Barr Virus Has Two Essential Functions Dependent on the Epigenetic State of the Viral Genome.” *Proceedings of the National Academy of Sciences* 107 (2): 850–55. <https://doi.org/10.1073/pnas.0911948107>.
- Kang, Hyojeung, and Paul M. Lieberman. 2009. “Cell Cycle Control of Kaposi’s Sarcoma-Associated Herpesvirus Latency Transcription by CTCF-Cohesin Interactions.” *Journal of Virology* 83 (12): 6199–6210. <https://doi.org/10.1128/JVI.00052-09>.
- Kang, Hyojeung, Andreas Wiedmer, Yan Yuan, Erle Robertson, and Paul M. Lieberman. 2011. “Coordination of KSHV Latent and Lytic Gene Control by CTCF-Cohesin Mediated Chromosome Conformation.” Edited by Samuel H. Speck. *PLoS Pathogens* 7 (8): e1002140. <https://doi.org/10.1371/journal.ppat.1002140>.
- Khan, Gulfaraz, and Muhammad Jawad Hashim. 2014. “Global Burden of Deaths from Epstein-Barr Virus Attributable Malignancies 1990-2010.” *Infectious Agents and Cancer* 9 (1): 38. <https://doi.org/10.1186/1750-9378-9-38>.
- Kim, Do Nyun, Min Koo Seo, Hoyun Choi, Su Yeon Kim, Hee Jong Shin, A-Ran Yoon, Qian Tao, Sun Young Rha, and Suk Kyeong Lee. 2013. “Characterization of Naturally Epstein–Barr Virus-Infected Gastric Carcinoma Cell Line YCCEL1.” *Journal of General Virology* 94 (3): 497–506. <https://doi.org/10.1099/vir.0.045237-0>.

- Kim, Kyoung-Dong, Hideki Tanizawa, Alessandra De Leo, Olga Vladimirova, Andrew Kossenkov, Fang Lu, Louise C. Showe, Ken-ichi Noma, and Paul M. Lieberman. 2020. "Epigenetic Specifications of Host Chromosome Docking Sites for Latent Epstein-Barr Virus." *Nature Communications* 11 (1): 877. <https://doi.org/10.1038/s41467-019-14152-8>.
- Kintner, C, and B Sugden. 1981. "Conservation and Progressive Methylation of Epstein-Barr Viral DNA Sequences in Transformed Cells." *Journal of Virology* 38 (1): 305–16. <https://doi.org/10.1128/jvi.38.1.305-316.1981>.
- Kojic, Aleksandar, Ana Cuadrado, Magali De Koninck, Daniel Giménez-Llorente, Miriam Rodríguez-Corsino, Gonzalo Gómez-López, François Le Dily, Marc A. Marti-Renom, and Ana Losada. 2018. "Distinct Roles of Cohesin-SA1 and Cohesin-SA2 in 3D Chromosome Organization." *Nature Structural & Molecular Biology* 25 (6): 496–504. <https://doi.org/10.1038/s41594-018-0070-4>.
- Kumar, Ashish, Yuanzhi Lyu, Yuichi Yanagihashi, Chanikarn Chantarasrivong, Vladimir Majerciak, Michelle Salemi, Kang-Hsin Wang, et al. 2022. "KSHV Episome Tethering Sites on Host Chromosomes and Regulation of Latency-Lytic Switch by CHD4." *Cell Reports* 39 (6): 110788. <https://doi.org/10.1016/j.celrep.2022.110788>.
- Langmead, Ben, and Steven L Salzberg. 2012. "Fast Gapped-Read Alignment with Bowtie 2." *Nature Methods* 9 (4): 357–59. <https://doi.org/10.1038/nmeth.1923>.
- Lareau, Caleb A, and Martin J Aryee. 2018. "Diffloop: A Computational Framework for Identifying and Analyzing Differential DNA Loops from Sequencing Data." Edited by Bonnie Berger. *Bioinformatics* 34 (4): 672–74. <https://doi.org/10.1093/bioinformatics/btx623>.
- Lareau, Caleb, and Martin Aryee. 2017. "Hichipper: A Preprocessing Pipeline for Assessing Library Quality and DNA Loops from HiChIP Data." Preprint. *Bioinformatics*. <https://doi.org/10.1101/192302>.
- Li, Bo, and Colin N Dewey. 2011. "RSEM: Accurate Transcript Quantification from RNA-Seq Data with or without a Reference Genome." *BMC Bioinformatics* 12 (1): 323. <https://doi.org/10.1186/1471-2105-12-323>.
- Li, Dajiang, Tim Mosbrugger, Dinesh Verma, and Sankar Swaminathan. 2020. "Complex Interactions between Cohesin and CTCF in Regulation of Kaposi's Sarcoma-

- Associated Herpesvirus Lytic Transcription.” Edited by Jae U. Jung. *Journal of Virology* 94 (2): e01279-19. <https://doi.org/10.1128/JVI.01279-19>.
- Li, Da-Jiang, Dinesh Verma, Tim Mosbrugger, and Sankar Swaminathan. 2014. “CTCF and Rad21 Act as Host Cell Restriction Factors for Kaposi’s Sarcoma-Associated Herpesvirus (KSHV) Lytic Replication by Modulating Viral Gene Transcription.” Edited by Paul Ling. *PLoS Pathogens* 10 (1): e1003880. <https://doi.org/10.1371/journal.ppat.1003880>.
- Li, Heng, and Richard Durbin. 2010. “Fast and Accurate Long-Read Alignment with Burrows–Wheeler Transform.” *Bioinformatics* 26 (5): 589–95. <https://doi.org/10.1093/bioinformatics/btp698>.
- Lin, Cheng-Te Major, Emily C. Leibovitch, M. Isabel Almira-Suarez, and Steven Jacobson. 2016. “Human Herpesvirus Multiplex ddPCR Detection in Brain Tissue from Low- and High-Grade Astrocytoma Cases and Controls.” *Infectious Agents and Cancer* 11 (1): 32. <https://doi.org/10.1186/s13027-016-0081-x>.
- Love, Michael I, Wolfgang Huber, and Simon Anders. 2014. “Moderated Estimation of Fold Change and Dispersion for RNA-Seq Data with DESeq2.” *Genome Biology* 15 (12): 550. <https://doi.org/10.1186/s13059-014-0550-8>.
- Lupey-Green, Lena N., Lisa B. Caruso, Jozef Madzo, Kayla A. Martin, Yinfei Tan, Michael Hulse, and Italo Tempera. 2018. “PARP1 Stabilizes CTCF Binding and Chromatin Structure To Maintain Epstein-Barr Virus Latency Type.” Edited by Jae U. Jung. *Journal of Virology* 92 (18): e00755-18. <https://doi.org/10.1128/JVI.00755-18>.
- Lupey-Green, Lena N., Stephanie A. Moquin, Kayla A. Martin, Shane M. McDevitt, Michael Hulse, Lisa B. Caruso, Richard T. Pomerantz, Jj L. Miranda, and Italo Tempera. 2017. “PARP1 Restricts Epstein Barr Virus Lytic Reactivation by Binding the BZLF1 Promoter.” *Virology* 507 (July): 220–30. <https://doi.org/10.1016/j.virol.2017.04.006>.
- Mach, Pia, Pavel I. Kos, Yinxiu Zhan, Julie Cramard, Simon Gaudin, Jana Tünnermann, Edoardo Marchi, et al. 2022. “Cohesin and CTCF Control the Dynamics of Chromosome Folding.” *Nature Genetics* 54 (12): 1907–18. <https://doi.org/10.1038/s41588-022-01232-7>.

- Martin, Kayla A., Lena N. Lupey, and Italo Tempera. 2016. "Epstein-Barr Virus Oncoprotein LMP1 Mediates Epigenetic Changes in Host Gene Expression through PARP1." Edited by J. U. Jung. *Journal of Virology* 90 (19): 8520–30. <https://doi.org/10.1128/JVI.01180-16>.
- Martínez, Francisco Puerta, Ruth Cruz, Fang Lu, Robert Plasschaert, Zhong Deng, Yisel A. Rivera-Molina, Marisa S. Bartolomei, Paul M. Lieberman, and Qiyi Tang. 2014. "CTCF Binding to the First Intron of the Major Immediate Early (MIE) Gene of Human Cytomegalovirus (HCMV) Negatively Regulates MIE Gene Expression and HCMV Replication." Edited by L. Hutt-Fletcher. *Journal of Virology* 88 (13): 7389–7401. <https://doi.org/10.1128/JVI.00845-14>.
- Martinez, Michael P., Xiaogang Cheng, Ancy Joseph, Jacob Al-Saleem, Amanda R. Panfil, Marilly Palettas, Wessel P. Dirksen, Lee Ratner, and Patrick L. Green. 2019. "HTLV-1 CTCF-Binding Site Is Dispensable for in Vitro Immortalization and Persistent Infection in Vivo." *Retrovirology* 16 (1): 44. <https://doi.org/10.1186/s12977-019-0507-9>.
- Masucci, M G, B Contreras-Salazar, E Ragnar, K Falk, J Minarovits, I Ernberg, and G Klein. 1989. "5-Azacytidine up Regulates the Expression of Epstein-Barr Virus Nuclear Antigen 2 (EBNA-2) through EBNA-6 and Latent Membrane Protein in the Burkitt's Lymphoma Line Rael." *Journal of Virology* 63 (7): 3135–41. <https://doi.org/10.1128/jvi.63.7.3135-3141.1989>.
- Mattiussi, Stefania, Italo Tempera, Giulia Matusali, Giulia Mearini, Luisa Lenti, Silvia Fratarcangeli, Luciana Mosca, Maria D'Erme, and Elena Mattia. 2007. "Inhibition of Poly(ADP-Ribose)Polymerase Impairs Epstein Barr Virus Lytic Cycle Progression." *Infectious Agents and Cancer* 2 (1): 18. <https://doi.org/10.1186/1750-9378-2-18>.
- Mehta, Kavi, Vignesh Gunasekharan, Ayano Satsuka, and Laimonis A. Laimins. 2015. "Human Papillomaviruses Activate and Recruit SMC1 Cohesin Proteins for the Differentiation-Dependent Life Cycle through Association with CTCF Insulators." Edited by Alison Anne McBride. *PLOS Pathogens* 11 (4): e1004763. <https://doi.org/10.1371/journal.ppat.1004763>.

- Messner, Simon, Matthias Altmeyer, Hongtao Zhao, Andrea Pozivil, Bernd Roschitzki, Peter Gehrig, Dorothea Rutishauser, Danzhi Huang, Amedeo Caflisch, and Michael O. Hottiger. 2010. "PARP1 ADP-Ribosylates Lysine Residues of the Core Histone Tails." *Nucleic Acids Research* 38 (19): 6350–62. <https://doi.org/10.1093/nar/gkq463>.
- Millau, Jean-François, and Luc Gaudreau. 2011. "CTCF, Cohesin, and Histone Variants: Connecting the Genome." *Biochemistry and Cell Biology* 89 (5): 505–13. <https://doi.org/10.1139/o11-052>.
- Morgan, Sarah M., Hideki Tanizawa, Lisa Beatrice Caruso, Michael Hulse, Andrew Kossenkov, Jozef Madzo, Kelsey Keith, et al. 2022. "The Three-Dimensional Structure of Epstein-Barr Virus Genome Varies by Latency Type and Is Regulated by PARP1 Enzymatic Activity." *Nature Communications* 13 (1): 187. <https://doi.org/10.1038/s41467-021-27894-1>.
- Mumbach, Maxwell R, Adam J Rubin, Ryan A Flynn, Chao Dai, Paul A Khavari, William J Greenleaf, and Howard Y Chang. 2016. "HiChIP: Efficient and Sensitive Analysis of Protein-Directed Genome Architecture." *Nature Methods* 13 (11): 919–22. <https://doi.org/10.1038/nmeth.3999>.
- Murphy, Gwen, Ruth Pfeiffer, M. Constanza Camargo, and Charles S. Rabkin. 2009. "Meta-Analysis Shows That Prevalence of Epstein–Barr Virus-Positive Gastric Cancer Differs Based on Sex and Anatomic Location." *Gastroenterology* 137 (3): 824–33. <https://doi.org/10.1053/j.gastro.2009.05.001>.
- Naseem, Madiha, Afsaneh Barzi, Christine Brezden-Masley, Alberto Puccini, Martin D. Berger, Ryuma Tokunaga, Francesca Battaglin, et al. 2018. "Outlooks on Epstein-Barr Virus Associated Gastric Cancer." *Cancer Treatment Reviews* 66 (May): 15–22. <https://doi.org/10.1016/j.ctrv.2018.03.006>.
- Nasmyth, Kim, Jan-Michael Peters, and Frank Uhlmann. 2000. "Splitting the Chromosome: Cutting the Ties That Bind Sister Chromatids." *Science* 288 (5470): 1379–84. <https://doi.org/10.1126/science.288.5470.1379>.
- Nonkwelo, C, J Skinner, A Bell, A Rickinson, and J Sample. 1996. "Transcription Start Sites Downstream of the Epstein-Barr Virus (EBV) Fp Promoter in Early-Passage Burkitt Lymphoma Cells Define a Fourth Promoter for Expression of the EBV

- EBNA-1 Protein.” *Journal of Virology* 70 (1): 623–27. <https://doi.org/10.1128/jvi.70.1.623-627.1996>.
- Oh, Sang Taek, Jung Seon Seo, Uk Yeol Moon, Kyeong Hee Kang, Dong-Jik Shin, Sungjoo Kim Yoon, Woo Ho Kim, Jae-Gahb Park, and Suk Kyeong Lee. 2004. “A Naturally Derived Gastric Cancer Cell Line Shows Latency I Epstein–Barr Virus Infection Closely Resembling EBV-Associated Gastric Cancer.” *Virology* 320 (2): 330–36. <https://doi.org/10.1016/j.virol.2003.12.005>.
- Okabe, Atsushi, Kie Kyon Huang, Keisuke Matsusaka, Masaki Fukuyo, Manjie Xing, Xuewen Ong, Takayuki Hoshii, et al. 2020. “Cross-Species Chromatin Interactions Drive Transcriptional Rewiring in Epstein–Barr Virus–Positive Gastric Adenocarcinoma.” *Nature Genetics* 52 (9): 919–30. <https://doi.org/10.1038/s41588-020-0665-7>.
- Palermo, Richard D., Helen M. Webb, and Michelle J. West. 2011. “RNA Polymerase II Stalling Promotes Nucleosome Occlusion and pTEFb Recruitment to Drive Immortalization by Epstein-Barr Virus.” Edited by Paul M. Lieberman. *PLoS Pathogens* 7 (10): e1002334. <https://doi.org/10.1371/journal.ppat.1002334>.
- Paris, Christian, Ieisha Pentland, Ian Groves, David C. Roberts, Simon J. Powis, Nicholas Coleman, Sally Roberts, and Joanna L. Parish. 2015. “CCCTC-Binding Factor Recruitment to the Early Region of the Human Papillomavirus 18 Genome Regulates Viral Oncogene Expression.” Edited by M. J. Imperiale. *Journal of Virology* 89 (9): 4770–85. <https://doi.org/10.1128/JVI.00097-15>.
- Pentland, Ieisha, Karen Campos-León, Marius Cotic, Kelli-Jo Davies, C. David Wood, Ian J. Groves, Megan Burley, et al. 2018. “Disruption of CTCF-YY1–Dependent Looping of the Human Papillomavirus Genome Activates Differentiation-Induced Viral Oncogene Transcription.” Edited by Bill Sugden. *PLOS Biology* 16 (10): e2005752. <https://doi.org/10.1371/journal.pbio.2005752>.
- Phillips, Jennifer E., and Victor G. Corces. 2009. “CTCF: Master Weaver of the Genome.” *Cell* 137 (7): 1194–1211. <https://doi.org/10.1016/j.cell.2009.06.001>.
- Preston-Alp, Sarah, Lisa Beatrice Caruso, Chenhe Su, Kelsey Keith, Samantha S. Soldan, Davide Maestri, Jozef Madzo, et al. 2023. “Decitabine Disrupts EBV Genomic Epiallele DNA Methylation Patterns around CTCF Binding Sites to

- Increase Chromatin Accessibility and Lytic Transcription in Gastric Cancer.” Edited by Blossom Damania. *mBio*, August, e00396-23. <https://doi.org/10.1128/mbio.00396-23>.
- Price, Alexander M., and Micah A. Luftig. 2015. “To Be or Not IIb: A Multi-Step Process for Epstein-Barr Virus Latency Establishment and Consequences for B Cell Tumorigenesis.” Edited by Richard C. Condit. *PLOS Pathogens* 11 (3): e1004656. <https://doi.org/10.1371/journal.ppat.1004656>.
- Price, Alexander M., Jason P. Tourigny, Eleonora Forte, Raul E. Salinas, Sandeep S. Dave, and Micah A. Luftig. 2012. “Analysis of Epstein-Barr Virus-Regulated Host Gene Expression Changes through Primary B-Cell Outgrowth Reveals Delayed Kinetics of Latent Membrane Protein 1-Mediated NF- $\kappa$ B Activation.” *Journal of Virology* 86 (20): 11096–106. <https://doi.org/10.1128/JVI.01069-12>.
- Ramírez, Fidel, Devon P Ryan, Björn Grüning, Vivek Bhardwaj, Fabian Kilpert, Andreas S Richter, Steffen Heyne, Friederike Dünder, and Thomas Manke. 2016. “deepTools2: A next Generation Web Server for Deep-Sequencing Data Analysis.” *Nucleic Acids Research* 44 (W1): W160–65. <https://doi.org/10.1093/nar/gkw257>.
- Rao, Suhas S.P., Miriam H. Huntley, Neva C. Durand, Elena K. Stamenova, Ivan D. Bochkov, James T. Robinson, Adrian L. Sanborn, et al. 2014. “A 3D Map of the Human Genome at Kilobase Resolution Reveals Principles of Chromatin Looping.” *Cell* 159 (7): 1665–80. <https://doi.org/10.1016/j.cell.2014.11.021>.
- Reisman, D, and B Sugden. 1986. “Trans Activation of an Epstein-Barr Viral Transcriptional Enhancer by the Epstein-Barr Viral Nuclear Antigen 1.” *Molecular and Cellular Biology* 6 (11): 3838–46. <https://doi.org/10.1128/MCB.6.11.3838>.
- Robertson, Keith D., S. Diane Hayward, Paul D. Ling, Dvorit Samid, and Richard F. Ambinder. 1995. “Transcriptional Activation of the Epstein-Barr Virus Latency C Promoter after 5-Azacytidine Treatment: Evidence That Demethylation at a Single CpG Site Is Crucial.” *Molecular and Cellular Biology* 15 (11): 6150–59. <https://doi.org/10.1128/MCB.15.11.6150>.
- Rooney, C M, M Brimmell, M Buschle, G Allan, P J Farrell, and J L Kolman. 1992. “Host Cell and EBNA-2 Regulation of Epstein-Barr Virus Latent-Cycle Promoter Activity

- in B Lymphocytes.” *Journal of Virology* 66 (1): 496–504. <https://doi.org/10.1128/jvi.66.1.496-504.1992>.
- Rowe, M, A L Lear, D Croom-Carter, A H Davies, and A B Rickinson. 1992. “Three Pathways of Epstein-Barr Virus Gene Activation from EBNA1-Positive Latency in B Lymphocytes.” *Journal of Virology* 66 (1): 122–31. <https://doi.org/10.1128/jvi.66.1.122-131.1992>.
- Rowley, M. Jordan, and Victor G. Corces. 2018. “Organizational Principles of 3D Genome Architecture.” *Nature Reviews Genetics* 19 (12): 789–800. <https://doi.org/10.1038/s41576-018-0060-8>.
- Sample, J, E B Henson, and C Sample. 1992. “The Epstein-Barr Virus Nuclear Protein 1 Promoter Active in Type I Latency Is Autoregulated.” *Journal of Virology* 66 (8): 4654–61. <https://doi.org/10.1128/jvi.66.8.4654-4661.1992>.
- Servant, Nicolas, Nelle Varoquaux, Bryan R. Lajoie, Eric Viara, Chong-Jian Chen, Jean-Philippe Vert, Edith Heard, Job Dekker, and Emmanuel Barillot. 2015. “HiC-Pro: An Optimized and Flexible Pipeline for Hi-C Data Processing.” *Genome Biology* 16 (1): 259. <https://doi.org/10.1186/s13059-015-0831-x>.
- Shannon-Lowe, Claire, and Alan Rickinson. 2019. “The Global Landscape of EBV-Associated Tumors.” *Frontiers in Oncology* 9 (August): 713. <https://doi.org/10.3389/fonc.2019.00713>.
- Smatti, Maria K., Duaa W. Al-Sadeq, Nadima H. Ali, Gianfranco Pintus, Haissam Abou-Saleh, and Gheyath K. Nasrallah. 2018. “Epstein–Barr Virus Epidemiology, Serology, and Genetic Variability of LMP-1 Oncogene Among Healthy Population: An Update.” *Frontiers in Oncology* 8 (June): 211. <https://doi.org/10.3389/fonc.2018.00211>.
- Stanland, Lyla J., and Micah A. Luftig. 2020. “The Role of EBV-Induced Hypermethylation in Gastric Cancer Tumorigenesis.” *Viruses* 12 (11): 1222. <https://doi.org/10.3390/v12111222>.
- Stedman, William, Hyojeung Kang, Shu Lin, Joseph L Kissil, Marisa S Bartolomei, and Paul M Lieberman. 2008. “Cohesins Localize with CTCF at the KSHV Latency Control Region and at Cellular C-Myc and H19/Igf2 Insulators.” *The EMBO Journal* 27 (4): 654–66. <https://doi.org/10.1038/emboj.2008.1>.

- Takacs, Maria, Ferenc Banati, Anita Koroknai, Judit Segesdi, Daniel Salamon, Hans Wolf, Hans Helmut Niller, and Janos Minarovits. 2010. "Epigenetic Regulation of Latent Epstein–Barr Virus Promoters." *Biochimica et Biophysica Acta (BBA) - Gene Regulatory Mechanisms* 1799 (3–4): 228–35. <https://doi.org/10.1016/j.bbagr.2009.10.005>.
- Tao, Qian, Keith D. Robertson, Angela Manns, Allan Hildesheim, and Richard F. Ambinder. 1998. "The Epstein-Barr Virus Major Latent Promoter Qp Is Constitutively Active, Hypomethylated, and Methylation Sensitive." *Journal of Virology* 72 (9): 7075–83. <https://doi.org/10.1128/JVI.72.9.7075-7083.1998>.
- Tempera, Italo, Zhong Deng, Constandache Atanasiu, Chi-Ju Chen, Maria D'Erme, and Paul M. Lieberman. 2010. "Regulation of Epstein-Barr Virus OriP Replication by Poly(ADP-Ribose) Polymerase 1." *Journal of Virology* 84 (10): 4988–97. <https://doi.org/10.1128/JVI.02333-09>.
- Tempera, Italo, Michael Klichinsky, and Paul M. Lieberman. 2011. "EBV Latency Types Adopt Alternative Chromatin Conformations." Edited by Jae U. Jung. *PLoS Pathogens* 7 (7): e1002180. <https://doi.org/10.1371/journal.ppat.1002180>.
- Tempera, Italo, and Paul M. Lieberman. 2010. "Chromatin Organization of Gammaherpesvirus Latent Genomes." *Biochimica et Biophysica Acta (BBA) - Gene Regulatory Mechanisms* 1799 (3–4): 236–45. <https://doi.org/10.1016/j.bbagr.2009.10.004>.
- . 2014. "Epigenetic Regulation of EBV Persistence and Oncogenesis." *Seminars in Cancer Biology* 26 (June): 22–29. <https://doi.org/10.1016/j.semcancer.2014.01.003>.
- Tempera, Italo, Andreas Wiedmer, Jayaraju Dheekollu, and Paul M. Lieberman. 2010. "CTCF Prevents the Epigenetic Drift of EBV Latency Promoter Qp." Edited by Blossom Damania. *PLoS Pathogens* 6 (8): e1001048. <https://doi.org/10.1371/journal.ppat.1001048>.
- The Cancer Genome Atlas Research Network. 2014. "Comprehensive Molecular Characterization of Gastric Adenocarcinoma." *Nature* 513 (7517): 202–9. <https://doi.org/10.1038/nature13480>.

- Thorley-Lawson, David A., and Andrew Gross. 2004. "Persistence of the Epstein–Barr Virus and the Origins of Associated Lymphomas." *New England Journal of Medicine* 350 (13): 1328–37. <https://doi.org/10.1056/NEJMra032015>.
- Thorley-Lawson, David A, Jared B Hawkins, Sean I Tracy, and Michael Shapiro. 2013. "The Pathogenesis of Epstein–Barr Virus Persistent Infection." *Current Opinion in Virology* 3 (3): 227–32. <https://doi.org/10.1016/j.coviro.2013.04.005>.
- Trivedi, Pankaj, Paola Spinsanti, Laura Cuomo, Massimo Volpe, Kenzo Takada, Luigi Frati, and Alberto Faggioni. 2001. "Differential Regulation of Epstein-Barr Virus (EBV) Latent Gene Expression in Burkitt Lymphoma Cells Infected with a Recombinant EBV Strain." *Journal of Virology* 75 (10): 4929–35. <https://doi.org/10.1128/JVI.75.10.4929-4935.2001>.
- Truong, Camtu D, Wei Feng, Wei Li, T Khoury, Q Li, S Alrawi, Yingyan Yu, Keping Xie, James Yao, and Dongfeng Tan. 2009. "Characteristics of Epstein-Barr Virus-Associated Gastric Cancer: A Study of 235 Cases at a Comprehensive Cancer Center in U.S.A." *Journal of Experimental & Clinical Cancer Research* 28 (1): 14. <https://doi.org/10.1186/1756-9966-28-14>.
- Wang, F, C D Gregory, M Rowe, A B Rickinson, D Wang, M Birkenbach, H Kikutani, T Kishimoto, and E Kieff. 1987. "Epstein-Barr Virus Nuclear Antigen 2 Specifically Induces Expression of the B-Cell Activation Antigen CD23." *Proceedings of the National Academy of Sciences* 84 (10): 3452–56. <https://doi.org/10.1073/pnas.84.10.3452>.
- Wang, F, S F Tsang, M G Kurilla, J I Cohen, and E Kieff. 1990. "Epstein-Barr Virus Nuclear Antigen 2 Transactivates Latent Membrane Protein LMP1." *Journal of Virology* 64 (7): 3407–16. <https://doi.org/10.1128/jvi.64.7.3407-3416.1990>.
- Wang, Kai, Junsuo Kan, Siu Tsan Yuen, Stephanie T Shi, Kent Man Chu, Simon Law, Tsun Leung Chan, et al. 2011. "Exome Sequencing Identifies Frequent Mutation of ARID1A in Molecular Subtypes of Gastric Cancer." *Nature Genetics* 43 (12): 1219–23. <https://doi.org/10.1038/ng.982>.
- Wang, Kai, Siu Tsan Yuen, Jiangchun Xu, Siu Po Lee, Helen H N Yan, Stephanie T Shi, Hoi Cheong Siu, et al. 2014. "Whole-Genome Sequencing and Comprehensive

- Molecular Profiling Identify New Driver Mutations in Gastric Cancer.” *Nature Genetics* 46 (6): 573–82. <https://doi.org/10.1038/ng.2983>.
- Washington, Shannan D., Samantha I. Edenfield, Caroline Lieux, Zachary L. Watson, Sean M. Taasan, Adit Dhummakupt, David C. Bloom, and Donna M. Neumann. 2018. “Depletion of the Insulator Protein CTCF Results in Herpes Simplex Virus 1 Reactivation *In Vivo*.” Edited by Rozanne M. Sandri-Goldin. *Journal of Virology* 92 (11): e00173-18. <https://doi.org/10.1128/JVI.00173-18>.
- Washington, Shannan D., Farhana Musarrat, Monica K. Ertel, Gregory L. Backes, and Donna M. Neumann. 2018. “CTCF Binding Sites in the Herpes Simplex Virus 1 Genome Display Site-Specific CTCF Occupation, Protein Recruitment, and Insulator Function.” Edited by Rozanne M. Sandri-Goldin. *Journal of Virology* 92 (8): e00156-18. <https://doi.org/10.1128/JVI.00156-18>.
- Watson, Zachary L., Shannan D. Washington, Dane M. Phelan, Alfred S. Lewin, Sonal S. Tuli, Gregory S. Schultz, Donna M. Neumann, and David C. Bloom. 2018. “*In Vivo* Knockdown of the Herpes Simplex Virus 1 Latency-Associated Transcript Reduces Reactivation from Latency.” Edited by Rozanne M. Sandri-Goldin. *Journal of Virology* 92 (16): e00812-18. <https://doi.org/10.1128/JVI.00812-18>.
- Woellmer, Anne, Jose M. Arteaga-Salas, and Wolfgang Hammerschmidt. 2012. “BZLF1 Governs CpG-Methylated Chromatin of Epstein-Barr Virus Reversing Epigenetic Repression.” Edited by Samuel H. Speck. *PLoS Pathogens* 8 (9): e1002902. <https://doi.org/10.1371/journal.ppat.1002902>.
- Woisetschlaeger, M, C N Yandava, L A Furmanski, J L Strominger, and S H Speck. 1990. “Promoter Switching in Epstein-Barr Virus during the Initial Stages of Infection of B Lymphocytes.” *Proceedings of the National Academy of Sciences* 87 (5): 1725–29. <https://doi.org/10.1073/pnas.87.5.1725>.
- Wong, Yide, Michael T. Meehan, Scott R. Burrows, Denise L. Doolan, and John J. Miles. 2022. “Estimating the Global Burden of Epstein–Barr Virus-Related Cancers.” *Journal of Cancer Research and Clinical Oncology* 148 (1): 31–46. <https://doi.org/10.1007/s00432-021-03824-y>.
- Young, Lawrence S., and Alan B. Rickinson. 2004. “Epstein–Barr Virus: 40 Years On.” *Nature Reviews Cancer* 4 (10): 757–68. <https://doi.org/10.1038/nrc1452>.

- Young, Lawrence S., Lee Fah Yap, and Paul G. Murray. 2016. "Epstein–Barr Virus: More than 50 Years Old and Still Providing Surprises." *Nature Reviews Cancer* 16 (12): 789–802. <https://doi.org/10.1038/nrc.2016.92>.
- Yu, Wenqiang, Vasudeva Ginja, Vinod Pant, Igor Chernukhin, Joanne Whitehead, France Docquier, Dawn Farrar, et al. 2004. "Poly(ADP-Ribosyl)ation Regulates CTCF-Dependent Chromatin Insulation." *Nature Genetics* 36 (10): 1105–10. <https://doi.org/10.1038/ng1426>.
- Zhang, Kai, Nan Li, Richard I. Ainsworth, and Wei Wang. 2016. "Systematic Identification of Protein Combinations Mediating Chromatin Looping." *Nature Communications* 7 (1): 12249. <https://doi.org/10.1038/ncomms12249>.
- Zhang, Shu, Nadine Übelmesser, Mariano Barbieri, and Argyris Papantonis. 2023. "Enhancer–Promoter Contact Formation Requires RNAPII and Antagonizes Loop Extrusion." *Nature Genetics* 55 (5): 832–40. <https://doi.org/10.1038/s41588-023-01364-4>.
- Zhang, Yong, Tao Liu, Clifford A Meyer, Jérôme Eeckhoute, David S Johnson, Bradley E Bernstein, Chad Nusbaum, et al. 2008. "Model-Based Analysis of ChIP-Seq (MACS)." *Genome Biology* 9 (9): R137. <https://doi.org/10.1186/gb-2008-9-9-r137>.